Journal of Sound and Vibration 325 (2009) 686–704

Contents lists available at ScienceDirect

Journal of Sound and Vibration

journal homepage: www.elsevier.com/locate/jsvi

Parametric instability regions of a soft and magnetorheological elastomer cored sandwich beam

S.K. Dwivedy *, N. Mahendra, K.C. Sahu

Mechanical Engineering Department, Indian Institute of Technology, Guwahati 781 039, India

ARTICLE INFO

Article history:
Received 7 March 2008
Received in revised form
10 February 2009
Accepted 27 March 2009
Handling Editor: L.G. Tham
Available online 20 May 2009

ABSTRACT

Present work deals with the study of parametric instability regions of a three-layered, symmetric sandwich beam with conductive skins subjected to periodic axial load. In the core layer, a magnetorheological elastomer (MRE) patch is placed in between two soft viscoelastic patches. The governing equations of motion of the system have been derived, and the parametric instability regions for simple and combination resonances have been investigated for simply supported, clamped–pinned, clamped–guided, and clamped–free end conditions by modified Hsu's method. The instability regions of the system with and without MRE patch, with different magnetic field strengths and permeability of skin materials have been studied. The advantages of using MRE to actively control the vibration of the sandwich beam have been demonstrated.

1. Introduction

Sandwich structures are very popular in aerospace and in many other industries due to their light weight and high-energy absorption properties. They provide many advantages such as high-specific stiffness, good buckling resistance, easy reparability, and high-corrosion resistance. The most important advantage is that optimal designs can be obtained for different applications by choosing different materials and geometric configurations of the face sheets and cores. One of such material to improve the design of sandwich beam is the use of magnetorheological elastomer (MRE) as core material. Magnetorheological elastomers comprise of a class of smart materials whose rheological properties can be controlled rapidly and reversibly by the application of an external magnetic field.

Most of the studies of sandwich structure [1–3] are devoted to the free vibration analysis considering classical theory or the anti-plane concept which implies that the deflections of the upper and lower faces are equal, and the longitudinal displacement distribution throughout the height of the core is linear. However, the classical theory is no longer valid when one uses foam-like core material [4] and hence, a higher order theory is used which takes both the nonlinear displacement fields of the core material and realistic supports into account. Frostig and Baruch [5] and Frostig [6] used this theory to study the behavior of a symmetric and non-symmetric sandwich beam with a flexible core.

In many applications these sandwich structures are subjected to parametric excitation, where a small excitation can produce a large response when the frequency of the excitation is closer to twice the natural frequencies (*principal parametric resonance*) or combination of different modal frequencies (*combination resonances*). The study of parametric instability is well known and can be found in detail in various textbooks, e.g., [7,8]. One may use several methods to study the parametric instability regions. Saito and Otomi [9] modified Hsu's [10] procedure to determine the stability of

* Corresponding author. Tel.: +91 361 258 2670; fax: +91 361 2690762.
E-mail address: dwivedy@iitg.ernet.in (S.K. Dwivedy).

0022-460X/$ - see front matter © 2009 Elsevier Ltd. All rights reserved.
doi:10.1016/j.jsv.2009.03.039

viscoelastic beams with an attached mass and viscoelastic end supports under axial and tangential periodic loads. Kar and Sujata [11], Ray and Kar [12,13] studied the parametric instability regions for simple and combination resonances for different types of sandwich beams with viscoelastic core by using the modified Hsu's procedure. In these works classical sandwich beam theory were used, and the core was assumed to be rigid in transverse direction. Recently, Dwivedy et al. [14] studied the parametric instability regions of a three-layered soft-cored sandwich beam using higher order theory.

Sandwich beams with MRE cores possess field-controllable flexure rigidities due to the field-dependant shear modulus of the MRE core. MRE was first introduced by Shiga et al. [15] and Jolly et al. [16], when many researchers concentrated on magnetorheological fluid (MRF) and MRF-based damping devices. Carlson and Jolly [17] have shown that MRE is much like MRF, except for the fact that chain-like structures of MRE are developed during the curing process, while the chain-like structures of MRF are formed during operation. This difference makes the operating mechanism of these two types of materials totally different. Employing a dipole model and a finite element method, Davis [18] noticed the maximum change of the dynamic shear modulus of MRE is about 50% when the volume fraction is 27%. Zhou [19] reported that such a field-dependent characteristic of the shear modulus vanishes when the deformation frequency is above several hundred Hertz. Zhou and Wang [20,21] showed that the field-induced maximum relative change of the resonant frequencies, and the anti-resonant frequencies of MRE-based sandwich beams could approach 30%. From an analytical solution for a vibrating conductive beam, Zhou and Wang [20,22] found that the field-dependent stiffness of MRE-based sandwich beams with conductive skins, subjected to magnetoelastic loads, is dominated by the field-dependent shear property of the MRE core. To fabricate good natural rubber-based MREs with high modulus, Chen et al. [23] studied the influences of a variety of fabrication conditions such as matrix type, external magnetic flux density, temperature, plasticizer, and iron particles on the MREs performances. Zhang and Li [24] proposed a new effective permeability model of MRE with a novel structure, which is designed to improve field-dependent performance. Deng and Gong [25] used magnetorheological elastomer as adoptive tuned vibration absorber.

From the above literature it is apparent that no work has been reported to study the stability of soft-cored sandwich beam with MRE subjected to parametric excitation. So in this work an effort has been made to study parametric instability regions of a three-layered sandwich beam in which a part of the foam-core is replaced by MRE. The objective of using MRE patch is to increase the stiffness of the structure actively by using magnetic field. In the considered structure due to parametric excitation, when the axial load is very well below the critical Euler buckling load, the beam may fail due to transverse vibration. Hence, it is very important to study the stability under axial loading to obtain the magnitude and frequency at which the system becomes unstable by plotting the instability regions. By using MRE patch, an attempt has been made to show that the instability region can be actively altered, so that an unstable system without MRE patch may become stable with MRE patch.

The governing equation of motion of such a system is developed using higher order theory [5,6,14], and the parametric instability regions are determined for different boundary conditions. This study will be very much useful to the researchers/designers working in the field of active and passive vibration suppression of sandwich structures using magnetic field.

2. Modeling

Fig. 1 shows a symmetric simply supported, three-layered sandwich beam of length L and width b. In the middle layer, a magnetorheological elastomer patch is placed in between two patches of foam-like soft viscoelastic materials. The top, core, and bottom layer thicknesses are d_t, c, and d_b, respectively. The top and bottom skins have been subjected to axial periodic load $P(t) = P_0 + P_1 \cos \omega t$, where P_0 and P_1 are, respectively, the amplitudes of static and dynamic load; ω is the frequency of the applied load, and t is the time. The skin materials are considered to be conductive materials and a magnetic filed with strength B is applied to the sandwich beam. The MRE core is configured with the chain-like structures embedded in the material perpendicular to the skins. The applied magnetic field is parallel to such chain-like structures and is perpendicular to the skins. Under dynamic deformations, motion-induced eddy current will be generated on the skins. Thus, the magnetic field near the skins will be disturbed and magnetoelastic loads will be applied to the skins. As a

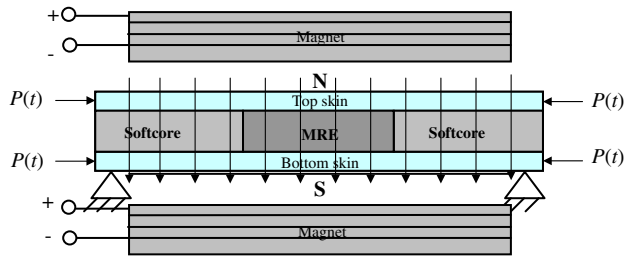

Fig. 1. Schematic diagram of a three-layered soft-cored sandwich beam with MRE patch subjected to periodic axial loading and magnetic field.

result, the bulk dynamic flexure rigidity is affected by the applied magnetic field through the field-dependant shear modulus of the MRE part of the core and the magnetomechanical coupling mechanism of the conductive skins.

The assumptions made for deriving the governing equations are similar to that by Frostig [6] and Dwivedy et al. [14], and are (i) the face sheets of the sandwich beam are modeled as Euler–Bernoulli beams, (ii) the transversely flexible core layer is considered as a two-dimensional elastic medium with small deformations where its height may change under loading, and its cross-section does not remain planar, and (iii) the longitudinal (in-plane) stresses in the core are neglected, and the interface layers between the face sheets and the core are assumed to be infinitely rigid and provide perfect continuity of the deformations at the interfaces.

The equation of motion is derived by using the extended Hamilton's principle, which is given by

$$\int_{t_1}^{t_2}(\delta L+\delta W_{\rm nc})\,{\rm d}t=0,\quad L=T-U, \tag{1}$$

where L is the Lagrangian of the system, T the kinetic energy, U the internal potential energy, $W_{\rm nc}$ the non-conservative work, δ the variational operator, t_1 and t_2 define the time interval, and t the time coordinate.

The kinetic energy of the system is

$$T=(1/2)\left\{\int_0^L m_t(\dot{u}_t^2+\dot{w}_t^2)\,{\rm d}x+\int_0^L m_b(\dot{u}_b^2+\dot{w}_b^2)\,{\rm d}x+\int_{v_{\rm core}}\rho_c\dot{u}_c^2\,{\rm d}v+\int_{v_{\rm core}}\rho_c\dot{w}_c^2\,{\rm d}v\right\}, \tag{2}$$

where m is the mass per unit length, u and w are the displacements in x and z directions, respectively; subscripts t, b, and c represent the top, bottom, and core layers, respectively; $(.)$ denotes the derivative with respect to time, and ρ_c the density of the core.

Based on higher order theory [6,14], the core is considered as a medium which transfers its inertial loads to the skins rather than resisting them by itself. Thus, it prevents the wave-like behavior in the vertical and horizontal directions of the core. The acceleration and the velocity in the vertical direction of the core are assumed to have the shape of the static deformation fields. In general, the static displacements field throughout the height of the core is nonlinear, especially in the vicinity of concentrated loads or supports. However, under uniformly distributed loads these nonlinearities are small and hence a linear distribution can be used. Thus, the displacement inside the core is given by

$$u_c=u_b+(d_b/2)w_{b,x}+u_t-\{(d_t/2)w_{t,x}\}\{1-(z/c)\},\quad w_c=(w_b-w_t)(z/c)+w_t. \tag{3}$$

The internal potential energy in terms of stress (σ) and strain (ε) is given by

$$U=\int_{v_{\rm top}}\sigma_{xx}\varepsilon_{xx}\,{\rm d}v+\int_{v_{\rm bot}}\sigma_{xx}\varepsilon_{xx}\,{\rm d}v+\int_{v_{\rm core}}\tau_c\gamma_c\,{\rm d}v+\int_{v_{\rm core}}\sigma_{zz}\varepsilon_{zz}\,{\rm d}v. \tag{4}$$

Here σ_{xx} and ε_{xx} are the longitudinal normal stress and strain in the upper and lower skins, respectively; τ_c and γ_c are shear stress and strain in the core, respectively; σ_{zz} and ε_{zz} are the vertical normal stress and strain in the core, respectively; $v_{\rm top}$, $v_{\rm bot}$, and $v_{\rm core}$ are the volumes of the upper and lower skins, and the core, respectively.

The non-conservative work is

$$W_{\rm nc}=(1/2)\int_0^L P(t)w_{q,x}^2\,{\rm d}x+\int_0^L[n_t\delta u_t+n_b\delta u_b+m_t^m\delta w_{t,x}+m_b^m\delta w_{b,x}]\,{\rm d}x, \tag{5}$$

where $()_{,x}=\partial()/\partial x$, n_j and m_j^m $(j=t,b)$ are the distributed equivalent horizontal force and moments induced by the magnetoelastic load on the top (t) and bottom (b) skins, respectively, and they can be expressed as [22]

$$n_j=\frac{B_0^2bd_j}{\mu_{ej}}u_{j,xx}, \tag{6}$$

$$m_j^m=m_j^{\rm Max}+m_j^{\rm Lor}=\frac{B_0^2bd_j}{\mu_0}\left[\frac{\pi}{2\,\ln(x/L-x)}u_{j,x}-\frac{d_j}{2\pi}\ln(x/L-x)w_{j,xx}+w_{j,x}\right]-\frac{B_0^2bd_j^3}{12\mu_{ej}}w_{j,xxx}. \tag{7}$$

Here, μ_{ej} $(j=t,b)$ is the permeability of the skins; μ_0 the permeability of free space, and B_0 the magnetic field strength which is applied in the transverse direction of the sandwich beam as shown in Fig. 1. In Eq. (7), $m_j^{\rm Max}$ represents the equivalent moment induced by Maxwell's stress jump at top $(j=t)$ and bottom $(j=b)$ skins, and $m_j^{\rm Lor}$ represents the equivalent moment induced by Lorenz body force at top $(j=t)$ and bottom $(j=b)$ skins.

Following non-dimensional parameters are used in the analysis:

$$\bar{P}_0=P_0L^2/(2E_qI_q),\quad \bar{P}_1=P_1L^2/(2E_qI_q),\quad \xi_c=G_c^*A_cL^2/E,\quad \phi_t=E_tA_tL^2/E,\quad \phi_b=E_bA_bL^2/E,$$

$$\phi_c=E_cA_cL^2/E,\quad g=G_c/(E_t(c/d_t)(L/d_t)^2+E_b(c/d_b)(L/d_b)^2),\quad \bar{t}=t/t_0,\quad \bar{x}=(x/L)$$

$$\bar{u}_q=(u_q/L),\quad \bar{w}_q=(w_q/L),\quad \bar{m}_q=(m_q/m),\quad \bar{m}_c=(m_c/m),\quad \bar{\omega}=\omega t_0. \tag{8}$$

Here $E=(E_tI_t+E_bI_b)$, $\bar{P}_0$ and $\bar{P}_1$ are the non-dimensional static and dynamic load amplitudes, respectively. E_q, I_q, and A_q are the Young's modulus, moment of inertia, and the area of cross-section of the qth (t or b) layer, respectively. E_c is the Young's modulus and A_c the area of cross-section for the core and, $t_0=(mL^4/E)^{(1/2)}$, where m is the total mass per unit length; m_c the mass of the core per unit length. $G_c^*=G_c(1+j\eta_c)$ is the complex shear modulus of the viscoelastic core, where G_c is the phase shear modulus, $j=\sqrt{-1}$, and η_c the core loss factor; and g the shear parameter.

Using, extended Hamilton's principle, the non-dimensional equations of motion are obtained as follows:

$$
\begin{aligned}
&\bar{m}_t\ddot{\bar{w}}_t+(1/3)(\bar{m}_cH_1+\bar{m}_rH_2)\ddot{\bar{w}}_t-(1/12)(d_t/c)^2(c/L)^2(\bar{m}_cH_1+\bar{m}_rH_2)\ddot{\bar{w}}_{t,\bar{x}\bar{x}}\\
&\quad+(1/576)(d_t/c)\{1+(d_t/c)\}(c/L)^4(\xi_c/\phi_c)(\bar{m}_cH_1+\bar{m}_rH_2)\ddot{\bar{w}}_{t,\bar{x}\bar{x}\bar{x}\bar{x}}\\
&\quad+(1/24)(d_t/c)(d_b/c)(c/L)^2(\bar{m}_cH_1+\bar{m}_rH_2)\ddot{\bar{w}}_{b,\bar{x}\bar{x}}\\
&\quad+(1/576)(d_b/c)\{1+(d_t/c)\}(c/L)^4(\bar{m}_c(\xi_c/\phi_c)H_1+\bar{m}_r(\xi_r/\phi_r)H_2)\ddot{\bar{w}}_{b,\bar{x}\bar{x}\bar{x}\bar{x}}\\
&\quad+(1/6)(\bar{m}_cH_1+\bar{m}_rH_2)\ddot{\bar{w}}_b+(1/6)(d_t/c)(c/L)(\bar{m}_cH_1+\bar{m}_rH_2)\ddot{\bar{u}}_{t,\bar{x}}\\
&\quad-(1/48)\bar{m}_t\{1+(d_t/c)\}(c/L)^3((\xi_c/\phi_c)H_1+(\xi_r/\phi_r)H_2)\ddot{\bar{u}}_{t,\bar{x}\bar{x}\bar{x}}\\
&\quad-(1/288)\{1+(d_t/c)\}(c/L)^3(\bar{m}_c(\xi_r/\phi_r)H_1+\bar{m}_r(\xi_r/\phi_r)H_2)\ddot{\bar{u}}_{t,\bar{x}\bar{x}\bar{x}}\\
&\quad+(1/12)(d_t/c)(c/L)(\bar{m}_cH_1+\bar{m}_rH_2)\ddot{\bar{u}}_{b,\bar{x}}\\
&\quad+(1/48)(\bar{m}_b)\{1+(d_t/c)\}(c/L)^3((\xi_c/\phi_c)H_1+(\xi_r/\phi_r)H_2)\ddot{\bar{u}}_{b,\bar{x}\bar{x}\bar{x}}\\
&\quad+(1/288)\{1+(d_t/c)\}(c/L)^3(\bar{m}_c(\xi_c/\phi_c)H_1+\bar{m}_r(\xi_r/\phi_r)H_2)\ddot{\bar{u}}_{b,\bar{x}\bar{x}\bar{x}}+\phi_c(L/c)^2\bar{w}_t\\
&\quad-(1/4)\{1+(d_t/c)^2\}((\xi_c/4)H_1+(\xi_r/4)H_2)\bar{w}_{t,\bar{x}\bar{x}}-\phi_c(L/c)^2\bar{w}_b\\
&\quad-(1/4)\{1+(d_t/c)\}\{1+(d_b/c)\}(\xi_cH_1+\xi_rH_2)\bar{w}_{b,\bar{x}\bar{x}}+(1/2)(L/c)\{1+(d_t/c)\}(\xi_cH_1+\xi_rH_2)\bar{u}_{t,\bar{x}}\\
&\quad+(\phi_t/48)(c/L)^3\{1+(d_t/c)\}((\xi_c/\phi_c)H_1+(\xi_r/\phi_r)H_2)\bar{u}_{t,\bar{x}\bar{x}\bar{x}\bar{x}\bar{x}}\\
&\quad-(1/2)(L/c)\{1+(d_t/c)\}(\xi_cH_1+\xi_rH_2)\bar{u}_{b,\bar{x}}\\
&\quad-(\phi_b/48)(c/L)^3\{1+(d_t/c)\}((\xi_c/\phi_c)H_1+(\xi_r/\phi_r)H_2)\bar{u}_{b,\bar{x}\bar{x}\bar{x}\bar{x}\bar{x}}\\
&\quad+(\phi_t/12)(d_t/c)^2(c/L)^2\bar{w}_{t,\bar{x}\bar{x}\bar{x}\bar{x}}+\bar{P}\bar{w}_{t,\bar{x}\bar{x}}+B_0^2bd_t^2L/(2\pi\mu_0E)(\ln(\bar{x}/(1-\bar{x})))_{,\bar{x}}\bar{w}_{t,\bar{x}\bar{x}}\\
&\quad+B_0^2bd_t^2L/(2\pi\mu_0E)\ln(\bar{x}/(1-\bar{x}))\bar{w}_{t,\bar{x}\bar{x}\bar{x}}-B_0^2bd_tL^2/(\mu_0E)\bar{w}_{t,\bar{x}\bar{x}}+B_0^2bd_t^3/(12E\mu_{et})\bar{w}_{t,\bar{x}\bar{x}\bar{x}\bar{x}}\\
&\quad-B_0^2bd_tL^2\pi/(2\mu_0E)(1/(\ln(\bar{x}/(1-\bar{x}))))_{,\bar{x}}\bar{u}_{t,\bar{x}}-B_0^2bd_tL^2/(2\mu_0E)\pi/(\ln(\bar{x}/(1-\bar{x})))\bar{u}_{t,\bar{x}\bar{x}}\\
&\quad-B_0^2bd_tc^3G_c/(48E_cEL)(1+d_t/c)\bar{u}_{t,\bar{x}\bar{x}\bar{x}\bar{x}}+B_0^2bd_bc^3G_c/(48E_cEL)(1+d_t/c)\bar{u}_{b,\bar{x}\bar{x}\bar{x}\bar{x}}=0,
\end{aligned}
\tag{9}
$$

$$
\begin{aligned}
&(1/6)(\bar{m}_cH_1+\bar{m}_rH_2)\ddot{\bar{w}}_t+(1/24)(d_t/c)(d_b/c)(c/L)^2(\bar{m}_cH_1+\bar{m}_rH_2)\ddot{\bar{w}}_{t,\bar{x}\bar{x}}\\
&\quad+(1/576)(d_t/c)\{1+(d_b/c)\}(c/L)^4(\bar{m}_c(\xi_c/\phi_c)H_1+\bar{m}_r(\xi_r/\phi_r)H_2)\ddot{\bar{w}}_{t,\bar{x}\bar{x}\bar{x}\bar{x}}+\bar{m}_b\ddot{\bar{w}}_b\\
&\quad+(1/3)(\bar{m}_cH_1+\bar{m}_rH_2)\ddot{\bar{w}}_b-(1/12)(d_t/c)^2(c/L)^2(\bar{m}_cH_1+\bar{m}_rH_2)\ddot{\bar{w}}_{b,\bar{x}\bar{x}}\\
&\quad+(1/576)(d_b/c)\{1+(d_b/c)\}(c/L)^4(\bar{m}_c(\xi_c/\phi_c)H_1+\bar{m}_r(\xi_r/\phi_r)H_2)\ddot{\bar{w}}_{b,\bar{x}\bar{x}\bar{x}\bar{x}}\\
&\quad-(1/12)(d_b/c)(c/L)(\bar{m}_cH_1+\bar{m}_rH_2)\ddot{\bar{u}}_{t,\bar{x}}-(1/48)\{1+(d_b/c)\}(c/L)^3\bar{m}_t((\xi_c/\phi_c)H_1\\
&\quad+(\xi_r/\phi_r)H_2)-(1/288)\{1+(d_b/c)\}(c/L)^3(\bar{m}_c(\xi_c/\phi_c)H_1+\bar{m}_r(\xi_r/\phi_r)H_2)\ddot{\bar{u}}_{t,\bar{x}\bar{x}\bar{x}}\\
&\quad-(1/6)(d_b/c)(c/L)(\bar{m}_cH_1+\bar{m}_rH_2)\ddot{\bar{u}}_{b,\bar{x}}\\
&\quad+(1/48)\{1+(d_b/c)\}(c/L)^3\bar{m}_b((\xi_c/\phi_c)H_1+(\xi_r/\phi_r)H_2)\ddot{\bar{u}}_{b,\bar{x}\bar{x}\bar{x}}\\
&\quad+(1/288)\{1+(d_b/c)\}(c/L)^3(\bar{m}_c(\xi_c/\phi_c)H_1+\bar{m}_r(\xi_r/\phi_r)H_2)\ddot{\bar{u}}_{b,\bar{x}\bar{x}\bar{x}}+\phi_c(L/c)^2\bar{w}_b\\
&\quad-(1/4)\{1+(d_t/c)\}\{1+(d_b/c)\}(\xi_cH_1+\xi_rH_2)\bar{w}_{t,\bar{x}\bar{x}}-(1/4)\{1+(d_b/c)\}^2(\xi_cH_1+\xi_rH_2)\bar{w}_{b,\bar{x}\bar{x}}\\
&\quad+(1/2)(L/c)\{1+(d_b/c)\}(\xi_cH_1+\xi_rH_2)\bar{u}_{t,\bar{x}}\\
&\quad+(\phi_t/48)\{1+(d_b/c)\}(c/L)^3((\xi_c/\phi_c)H_1+(\xi_r/\phi_r)H_2)\bar{u}_{t,\bar{x}\bar{x}\bar{x}\bar{x}\bar{x}}\\
&\quad-(1/2)(L/c)\{1+(d_b/c)\}(\xi_cH_1+\xi_rH_2)\bar{u}_{b,\bar{x}}-\phi_c(L/c)^2\bar{w}_t\\
&\quad-(\phi_b/48)\{1+(d_b/c)\}(c/L)^3((\xi_c/\phi_c)H_1+(\xi_r/\phi_r)H_2)\bar{u}_{b,\bar{x}\bar{x}\bar{x}\bar{x}\bar{x}}\\
&\quad+(\phi_b/12)(d_b/c)^2(c/L)^2\bar{w}_{b,\bar{x}\bar{x}\bar{x}\bar{x}}+\bar{P}\bar{w}_{b,\bar{x}\bar{x}}+B_0^2bd_b^2L/(2\pi\mu_0E)(\ln(\bar{x}/(1-\bar{x})))_{,\bar{x}}\bar{w}_{b,\bar{x}\bar{x}}\\
&\quad+B_0^2bd_b^2L/(2\pi\mu_0E)\ln(\bar{x}/(1-\bar{x}))\bar{w}_{b,\bar{x}\bar{x}\bar{x}}-B_0^2bd_bL^2/(\mu_0E)\bar{w}_{b,\bar{x}\bar{x}}+B_0^2bd_b^3/(12E\mu_{eb})\bar{w}_{b,\bar{x}\bar{x}\bar{x}\bar{x}}\\
&\quad-B_0^2bd_bL^2\pi/(2\mu_0E)(1/(\ln(\bar{x}/(1-\bar{x}))))_{,\bar{x}}\bar{u}_{b,\bar{x}}-B_0^2bd_bL^2/(2\mu_0E)\pi/(\ln(\bar{x}/(1-\bar{x})))\bar{u}_{b,\bar{x}\bar{x}}\\
&\quad-B_0^2bd_tc^3G_c/(48E_cEL)(1+d_b/c)\bar{u}_{t,\bar{x}\bar{x}\bar{x}\bar{x}}+B_0^2bd_bc^3G_c/(48E_cEL)(1+d_b/c)\bar{u}_{b,\bar{x}\bar{x}\bar{x}\bar{x}}=0,
\end{aligned}
\tag{10}
$$

$$
\begin{aligned}
&(1/6)(d_t/c)(c/L)(\bar{m}_c H_1+\bar{m}_r H_2)\ddot{\bar{w}}_{t,\bar{x}}-(1/288)(d_t/c)(c/L)^3(\bar{m}_c(\xi_c/\phi_c)H_1+\bar{m}_r(\xi_r/\phi_r)H_2)\ddot{\bar{w}}_{t,\overline{xxx}}\\
&-(1/12)(d_b/c)(c/L)(\bar{m}_c H_1+\bar{m}_r H_2)\ddot{\bar{w}}_{b,\bar{x}}-(1/288)(d_b/c)(c/L)^3(\bar{m}_c(\xi_c/\phi_c)H_1\\
&+\bar{m}_r(\xi_r/\phi_r)H_2)\ddot{\bar{w}}_{b,\overline{xxx}}+(1/24)(\bar{m}_t)(c/L)^2((\xi_c/\phi_c)H_1+(\xi_r/\phi_r)H_2)\ddot{\bar{u}}_{t,\overline{xx}}+(1/144)(c/L)^2(\bar{m}_c(\xi_c/\phi_c)H_1\\
&+\bar{m}_r(\xi_r/\phi_r)H_2)\ddot{\bar{u}}_{t,\overline{xx}}-(\bar{m}_t)\ddot{\bar{u}}_t-(1/3)(\bar{m}_c H_1+\bar{m}_r H_2)\ddot{\bar{u}}_t-(1/24)(c/L)^2\bar{m}_b((\xi_c/\phi_c)H_1+(\xi_r/\phi_r)H_2)\ddot{\bar{u}}_{b,\overline{xx}}\\
&-(1/144)(c/L)^2(\bar{m}_c(\xi_c/\phi_c)H_1+\bar{m}_r(\xi_r/\phi_r)H_2)\ddot{\bar{u}}_{b,\overline{xx}}-(\bar{m}_c/6)\ddot{\bar{u}}_b\\
&+(1/2)\{1+(d_t/c)\}(L/c)(\xi_c H_1+\xi_r H_2)\bar{w}_{t,\bar{x}}+(1/2)(L/c)\{1+(d_b/c)\}(\xi_c H_1+\xi_r H_2)\bar{w}_{b,\bar{x}}+\phi_t\bar{u}_{t,\overline{xx}}\\
&-(L/c)^2(\xi_c H_1+\xi_r H_2)\bar{u}_t-(\phi_t/24)(c/L)^2((\xi_c/\phi_c)H_1+(\xi_r/\phi_r)H_2)\bar{u}_{t,\overline{xxxx}}\\
&+(L/c)^2(\xi_c H_1+\xi_r H_2)\bar{u}_b+(\phi_b/24)(c/L)^2((\xi_c/\phi_c)H_1+(\xi_r/\phi_r)H_2)\bar{u}_{b,\overline{xxxx}}\\
&-B_0^2 b d_t L^2/(\mu_{et}E)\bar{u}_{t,\overline{xx}}+B_0^2 b d_t c^2 G_c/(24\mu_{et}EE_c)\bar{u}_{t,\overline{xxxx}}\\
&-B_0^2 b d_b c^2 G_c/((24\mu_{eb}EE_c))\bar{u}_{b,\overline{xxxx}}=0,
\end{aligned}
\tag{11}
$$

$$
\begin{aligned}
&(1/12)(d_t/c)(c/L)(\bar{m}_c H_1+\bar{m}_r H_2)\ddot{\bar{w}}_{t,\bar{x}}+(1/288)(d_t/c)(c/L)^3(\bar{m}_c(\xi_c/\phi_c)H_1+\bar{m}_r(\xi_r/\phi_r)H_2)\ddot{\bar{w}}_{t,\overline{xxx}}\\
&-(1/6)(d_b/c)(c/L)(\bar{m}_c H_1+\bar{m}_r H_2)\ddot{\bar{w}}_{b,\bar{x}}+(1/288)(d_b/c)(c/L)^3(\bar{m}_c(\xi_c/\phi_c)H_1\\
&+\bar{m}_r(\xi_r/\phi_r)H_2)\ddot{\bar{w}}_{b,\overline{xxx}}-(1/6)(\bar{m}_c H_1+\bar{m}_r H_2)\ddot{\bar{u}}_t-(1/24)(c/L)^2\bar{m}_t((\xi_c/\phi_c)H_1+(\xi_r/\phi_r)H_2)\ddot{\bar{u}}_{t,\overline{xx}}\\
&-(1/144)(c/L)^2(\bar{m}_c(\xi_c/\phi_c)H_1+\bar{m}_r(\xi_r/\phi_r)H_2)\ddot{\bar{u}}_{t,\overline{xx}}-(\bar{m}_b)\ddot{\bar{u}}_b-(1/3)(\bar{m}_c H_1+\bar{m}_r H_2)\ddot{\bar{u}}_b\\
&+(1/24)(\bar{m}_b)(c/L)^2((\xi_c/\phi_c)H_1+(\xi_r/\phi_r)H_2)\ddot{\bar{u}}_{b,\overline{xx}}\\
&+(1/144)(c/L)^2(\bar{m}_c(\xi_c/\phi_c)H_1\bar{m}_r(\xi_r/\phi_r)H_2)\ddot{\bar{u}}_{b,\overline{xx}}\\
&-(1/2)\{1+(d_t/c)\}(L/c)(\xi_c H_1+\xi_r H_2)\bar{w}_{t,\bar{x}}-(1/2)(L/c)\{1+(d_b/c)\}(\xi_c H_1+\xi_r H_2)\bar{w}_{b,\bar{x}}\\
&+(L/c)^2(\xi_c H_1+\xi_r H_2)\bar{u}_t+\phi_b\bar{u}_{b,\overline{xx}}+(\phi_t/24)(c/L)^2((\xi_c/\phi_c)H_1+(\xi_r/\phi_r)H_2)\bar{u}_{t,\overline{xxxx}}\\
&-(L/c)^2(\xi_c H_1+\xi_r H_2)\bar{u}_b-(\phi_b/24)(c/L)^2((\xi_c/\phi_c)H_1+(\xi_r/\phi_r)H_2)\bar{u}_{b,\overline{xxxx}}\\
&-B_0^2 b d_b L^2/(\mu_{eb}E)\bar{u}_{b,\overline{xx}}-B_0^2 b d_t c^2 G_c/(24\mu_{et}EE_c)\bar{u}_{t,\overline{xxxx}}+B_0^2 b d_b c^2 G_c/((24\mu_{eb}EE_c))\bar{u}_{b,\overline{xxxx}}=0.
\end{aligned}
\tag{12}
$$

For the sandwich beam with MRE placed in the middle of the core

$$
H_1=H(x)-H(x-L_1)+H(x-L_2),\quad H_2=H(x-L_1)-H(x-L_2).
\tag{13}
$$

Here $L_1=L/3$, $L_2=2L/3$, and H is the Heaviside function.

It may be noted that in the absence of MRE patch and magnetic field, the above equations of motion Eqs. (9)–(12) reduces to those obtained in the work of Dwivedy et al. [14]. Further, in the absence of periodic axial forcing these equations reduces to those of Frostig and Baruch [5]. Also, in the absence of axial periodic load, Eqs. (9)–(12) reduces to those obtained by Zhou and Wang [22].

3. Approximate solution

To obtain the temporal equations of motion, generalized Galerkin's method is used considering multimode discretization as follows:

$$
\bar{w}_t=\sum_{m=1}^{N}f_m(\bar{t})w_m(\bar{x}),\quad \bar{w}_b=\sum_{q=N+1}^{2N}f_q(\bar{t})w_q(\bar{x}),\quad \bar{u}_t=\sum_{r=2N+1}^{3N}f_r(\bar{t})u_r(\bar{x}),\quad \text{and}\quad \bar{u}_b=\sum_{s=3N+1}^{4N}f_s(\bar{t})u_s(\bar{x}).
\tag{14}
$$

Here N is a positive integer representing the number of modes taken in the analysis, $f_m(\bar{t})$, $f_q(\bar{t})$, $f_r(\bar{t})$, and $f_s(\bar{t})$ are the generalized coordinates; $w_m(\bar{x})$, $w_q(\bar{x})$, $u_r(\bar{x})$, and $u_s(\bar{x})$are the shape functions chosen to satisfy as many of the boundary conditions.

Replacing H_1 and H_2 by using Eq. (13) in Eqs. (9)–(12), and applying generalized Galerkin's principle the resulting temporal equation of motion becomes

$$
[\mathbf{M}]\{\ddot{f}\}+[\mathbf{K}]\{\mathbf{f}\}-\bar{P}_1\cos\bar{\omega}\bar{t}[\mathbf{H}]\{\mathbf{f}\}=\{\boldsymbol{\phi}\}.
\tag{15}
$$

Here $\{\mathbf{f}\}=\{\{f_1\}^{\mathrm{T}}\{f_2\}^{\mathrm{T}}\{f_3\}^{\mathrm{T}}\{f_4\}^{\mathrm{T}}\}^{\mathrm{T}}$, $\{\boldsymbol{\phi}\}$, and $[\boldsymbol{\phi}]$ are null matrices, and $(\cdot)=\mathrm{d}(\,)/\mathrm{d}\bar{t}$. Other coefficients are as follows:

$$
[\mathbf{M}]=\begin{bmatrix}[M_{11}] & [M_{12}] & [M_{13}] & [M_{14}]\\ [M_{21}] & [M_{22}] & [M_{23}] & [M_{24}]\\ [M_{31}] & [M_{32}] & [M_{33}] & [M_{34}]\\ [M_{41}] & [M_{42}] & [M_{43}] & [M_{44}]\end{bmatrix},\quad
[\mathbf{K}_1]=\begin{bmatrix}[K_{11}] & [K_{12}] & [K_{13}] & [K_{14}]\\ [K_{21}] & [K_{22}] & [K_{23}] & [K_{24}]\\ [K_{31}] & [K_{32}] & [K_{33}] & [K_{34}]\\ [K_{41}] & [K_{42}] & [K_{43}] & [K_{44}]\end{bmatrix},
$$

$$[\mathbf{F}]=\begin{bmatrix}[F_{11}] & [F_{12}] & [F_{13}] & [F_{14}]\\ [F_{21}] & [F_{22}] & [F_{23}] & [F_{24}]\\ [F_{31}] & [F_{32}] & [F_{33}] & [F_{34}]\\ [F_{41}] & [F_{42}] & [F_{43}] & [F_{44}]\end{bmatrix},\quad [\mathbf{H}]=\begin{bmatrix}[H_{11}] & [\phi] & [\phi] & [\phi]\\ [\phi] & [H_{22}] & [\phi] & [\phi]\\ [\phi] & [\phi] & [\phi] & [\phi]\\ [\phi] & [\phi] & [\phi] & [\phi]\end{bmatrix},$$

$$[\mathbf{K}_2]=[\mathbf{K}_1]+[\mathbf{F}]\quad\text{and}\quad[\mathbf{K}]=[\mathbf{K}_2]-\bar{P}_0[\mathbf{H}]. \tag{16}$$

The elements of various submatrices are given in Appendix A. Eq. (15) is a set of coupled Mathieu–Hill equations with complex coefficients. If [**L**] is a normalized modal matrix of $[\mathbf{M}]^{-1}[\mathbf{K}]$, then the linear transformation $\{\mathbf{f}\}=[\mathbf{L}]\{\mathbf{U}\}$, will transform Eq. (15) to

$$\ddot{U}_q+(\omega_q^*)^2U_q+2\varepsilon\cos\bar{\omega}\bar{t}\sum_{p=1}^{4N}b_{qp}^*U_p=0,\quad q=1\ldots4N, \tag{17}$$

where $(\omega_q^*)^2$ are the distinct eigen values of $[\mathbf{M}]^{-1}[\mathbf{K}]$, b_{qp}^* are the elements of $[\mathbf{B}]=-[\mathbf{L}]^{-1}[\mathbf{M}]^{-1}[\mathbf{H}][\mathbf{L}]$, and $\varepsilon=\bar{P}_1/2<1$ for the present analysis.

The complex frequency and forcing parameters in terms of real and imaginary parts are given by

$$\omega_q^*=\omega_{q,R}+\mathrm{j}\omega_{q,I},\quad b_{qp}^*=b_{qp,R}+\mathrm{j}b_{qp,I}. \tag{18}$$

Following shape functions are taken for numerical calculations. These shape functions are slight modifications of the shape functions taken in the work of Ray and Kar [12] and are similar to those presented in the work of Dwivedy et al. [14]. For completeness of the work, the shape functions of all the boundary conditions are written below.

For simply supported beam:

$$w_m(\bar{x})=\sin(m\pi\bar{x}),\quad w_q(\bar{x})=\sin(\bar{q}\pi\bar{x}),\quad u_r(\bar{x})=\cos(\bar{r}\pi\bar{x}),\quad u_s(\bar{x})=\cos(\bar{s}\pi\bar{x}), \tag{19}$$

where $\bar{q}=(q-N),\bar{r}=(r-2N)$, and $\bar{s}=(s-3N)$.

For clamped–pinned beam:

$$w_m(\bar{x})=2(m+2)\bar{x}^{(m+1)}-(4m+6)\bar{x}^{(m+2)}+2(m+1)\bar{x}^{(m+3)},$$

$$w_q(\bar{x})=2(\bar{q}+2)\bar{x}^{(\bar{q}+1)}-(4\bar{q}+6)\bar{x}^{(\bar{q}+2)}+2(\bar{q}+1)\bar{x}^{(\bar{q}+3)},$$

$$u_{\bar{r}}(\bar{x})=(\bar{r}+1)\bar{x}^{\bar{r}}-\bar{k}\bar{x}^{(\bar{r}+1)},\quad u_s(\bar{x})=(\bar{s}+1)\bar{x}^{\bar{s}}-\overline{sx}^{(\bar{s}+1)}. \tag{20}$$

For clamped–guided beam:

$$\begin{aligned}w_m(\bar{x})=&(m+3)(m+2)(m+1)\{2+(2-\mu_1)m\}\bar{x}^{(m+1)}-[2(m+3)(m+1)^2\{1+(2-\mu_1)m\}\\&+\mu_1(m+1)/\{2(m+2)+(2-\mu_1)(m+2)m\}]\bar{x}^{(m+2)}\\&+[(m+2)(m+1)^2m(2-\mu_1)-\mu_1m(m+1)/\{2(m+3)+(2-\mu_1)(m+3)m\}]\bar{x}^{(m+3)},\end{aligned}$$

$$\begin{aligned}w_q(\bar{x})=&(\bar{q}+3)(\bar{q}+2)(\bar{q}+1)\{2+(2-\mu_2)\bar{q}\}\bar{x}^{(\bar{q}+1)}-[2(\bar{q}+3)(\bar{q}+1)^2\{1+(2-\mu_2)\bar{q}\}\\&+\mu_2\{(\bar{q}+1)/\{2(\bar{q}+2)+(2-\mu_2)(\bar{q}+2)\bar{q}]\bar{x}^{(\bar{q}+2)}\\&+[(\bar{q}+2)(\bar{q}+1)^2q(2-\mu_2)-\mu_2\bar{q}(\bar{q}+1)/\{2(\bar{q}+3)+(2-\mu_2)(\bar{q}+3)q\}]\bar{x}^{(\bar{q}+3)},\end{aligned}$$

$$u_r(\bar{x})=(\bar{r}+1)\bar{x}^{r}-[2(\bar{r}+3)(\bar{r}+2)(\bar{r}+1)+\bar{r}\{1+\mu_1/(2+2\bar{r}-\mu_1\bar{r})\}]\bar{x}^{(\bar{r}+1)},$$

$$u_{\bar{s}}(\bar{x})=(s+1)\bar{x}^{\bar{s}}-[2(\bar{s}+3)(\bar{s}+2)(\bar{s}+1)+\bar{s}\{1+\mu_1/(2+2s-\mu_1\bar{s})\}]\bar{x}^{(\bar{s}+1)}, \tag{21}$$

where $\mu_1=Y/(1+Y)$, $Y=3(1+(c/dt)^2)$, $\mu_2=X/(1+X)$, and $X=3(1+(c/db)^2)$.

For clamped–free beam:

$$\begin{aligned}w_m(\bar{x})=&(m+3)(m+2)\{(m+2)(m+1)-\mu_2\}\bar{x}^{(m+1)}+[2(m+3)(m+1)\{\mu_2-m(m+2)\}\\&\times\mu_1m(m+1)/\{(m+2)(m+1)-\mu_2\}]+[(m+2)(m+1)\{-\mu_2+m(m+1)\}\\&-\mu_1m(m+1)^2/\{(m+3)(m+2)(m+1)-(m+3)\mu_2\}\bar{x}^{(m+3)},\end{aligned}$$

$$\begin{aligned}w_q(\bar{x})=&(\bar{q}+3)(\bar{q}+2)\{(\bar{q}+2)(\bar{q}+1)-\mu_2\}\bar{x}^{(\bar{q}+1)}+[2(\bar{q}+3)(\bar{q}+1)\{\mu_2-\bar{q}(\bar{q}+2)\}\\&\times\mu_1\bar{q}(\bar{q}+1)/\{(\bar{q}+2)(\bar{q}+1)-\mu_2\}]+[(\bar{q}+2)(\bar{q}+1)\{-\mu_2+\bar{q}(\bar{q}+1)\}\\&-\mu_1\bar{q}(\bar{q}+1)^2/\{(\bar{q}+3)(\bar{q}+2)(\bar{q}+1)-(\bar{q}+3)\mu_2\}\bar{x}^{(\bar{q}+3)},\end{aligned}$$

$$u_r(\bar{x})=(\bar{r}+1)x^{\bar{r}}-\overline{rx}^{(\bar{r}+1)},\quad u_s(\bar{x})=(\bar{s}+1)x^{\bar{r}}-\overline{sx}^{(\bar{s}+1)}. \tag{22}$$

4. Regions of instability

The boundaries of the regions of instability for simple and combination resonances are obtained by the modified Hsu's [10] method. When the system is excited at a frequency nearly equal to twice the natural frequencies principal parametric resonance and when it is excited near a frequency, which is equal to sum or differences of any two modal frequencies combination resonances of sum or difference types take place. Following relations have been used to obtain the boundaries of the regions of instability for simple and combination resonances [12,14].

(1) For principal parametric resonance case:

$$|(\bar{\omega}/2) - \omega_{\mu,R}| < \tfrac{1}{4}\chi_\mu, \quad \mu = 1,2,\ldots,4N, \tag{23}$$

where

$$\chi_\mu = \left[\frac{4\varepsilon^2(b_{\mu\mu,R}^2 + b_{\mu\mu,I}^2)}{\omega_{\mu,R}^2} - 16\omega_{\mu,I}^2\right]. \tag{24}$$

(2) For combination resonance of sum type:

$$|\bar{\omega} - (\omega_{\mu,R} + \omega_{\nu,R})| < \chi_{\mu\nu}. \tag{25}$$

In the presence of damping

$$\chi_{\mu\nu} = \frac{(\omega_{\mu,I} + \omega_{\nu,I})}{4(\omega_{\mu,I}\omega_{\nu,I})^{1/2}}\left[\frac{4\varepsilon^2(b_{\mu\nu,R}b_{\nu\mu,R} + b_{\mu\nu,I}b_{\nu\mu,I})}{\omega_{\mu,R}\omega_{\nu,R}} - 16\omega_{\mu,I}\omega_{\nu,I}\right]^{1/2} \tag{26}$$

and for the undamped case

$$\chi_{\mu\nu} = \varepsilon[b_{\mu\nu,R}b_{\nu\mu,R}/\omega_{\mu,R}b_{\nu,R}]^{1/2}, \quad \mu \neq \nu \;\; \mu = \nu = 1,2,\ldots,4N. \tag{27}$$

(3) For combination resonance of difference type:

$$|\bar{\omega} - (\omega_{\nu,R} - \omega_{\mu,R})| < \Lambda_{\mu\nu}, \quad \mu > \nu, \;\; \mu = \nu = 1,2,\ldots,4N. \tag{28}$$

In the presence of damping

$$\Lambda_{\mu\nu} = \frac{(\omega_{\mu,I} + \omega_{\nu,I})}{4(\omega_{\mu,I}\omega_{\nu,I})^{1/2}}\left[\frac{4\varepsilon^2(b_{\mu\nu,I}b_{\nu\mu,I} - b_{\mu\nu,R}b_{\nu\mu,R})}{\omega_{\mu,R}\omega_{\nu,R}} - 16\omega_{\mu,I}\omega_{\nu,I}\right]^{1/2} \tag{29}$$

and for the undamped case

$$\Lambda_{\mu\nu} = \varepsilon[-b_{\mu\nu,R}b_{\nu\mu,R}/\omega_{\mu,R}b_{\nu,R}]^{1/2}. \tag{30}$$

5. Results and discussions

Here the instability regions of a three-layered, soft-cored; symmetric sandwich beam with MRE for simply supported, clamped–pinned, clamped–guided, and clamped–free boundary conditions have been studied numerically using MATLAB. The results have been compared with a sandwich beam in which the middle layer is fully made of soft-core. In the parametric instability regions shown in the following figures, the regions enclosed by the curves are unstable and the regions outside the curves are stable. Here the ordinate $\bar{P}_1$ is the amplitude of non-dimensional dynamic load, and the abscissa $\bar{\omega}$ is the non-dimensional forcing frequency. Following physical parameters have been taken for the numerical analysis, which are similar to those taken by Zhou and Wang [22]. The span of the beam, $L = 150\,\text{mm}$; width, $b = 15\,\text{mm}$; the top and bottom face thickness, $d_t = d_b = 0.1\,\text{mm}$; the core thickness, $c = 2\,\text{mm}$; Young's modulus of the skins, $E_t = E_b = 72\,\text{GPa}$; the zero-field shear modulus of MRE and the shear modulus of non-MRE soft-core is 0.388 MPa; the Young's modulus of the MRE part which is assumed to be unchanged with the applied magnetic field and the non-MRE part is 1.7 MPa, the densities of the skins, $\rho_t = \rho_b = 2700\,\text{kg/m}^3$; the density of the core, including MRE part and the non-MRE part (ρ_c) is $1100\,\text{kg/m}^3$. The permeability of the vacuum, $\mu_0 = 1.26 \times 10^{-6}\,\text{H m}^{-1}$ and the relative permeability of the skin material is considered to be 1 for the instability regions plotted in Figs. 2–7. For Fig. 8, relative permeability of the skin materials have been taken as 10 similar to those taken in the work of Zhou and Wang [22]. Following the variation of shear modulus with magnetic field in the work of Deng and Gong [25], in this work, while for $B_0 = 0.6\,\text{T}$, the shear modulus of the MRE part has been considered to be 1.5 times that of zero-field shear modulus, for $B_0 = 0.8\,\text{T}$, the shear modulus of the MRE part has been taken as 1.55 times that of the zero-field shear modulus. The non-dimensional static loading $\bar{P}_0$ has been

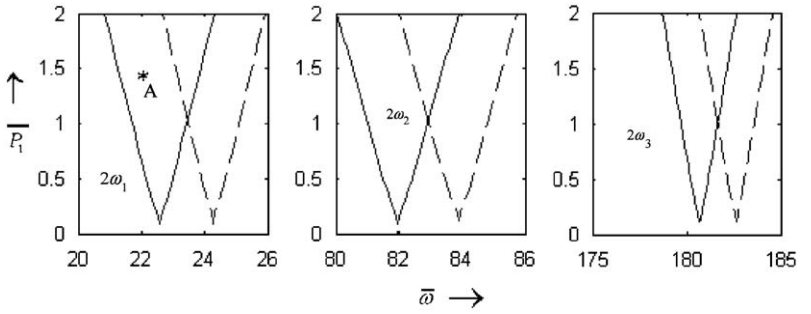

Fig. 2. Parametric instability regions of a simply supported sandwich beam for the first three modes of principal parametric resonance: ———, with only soft-core and - - - - - - -, with MRE placed in middle of soft-core. $\mu_r = 1.0$.

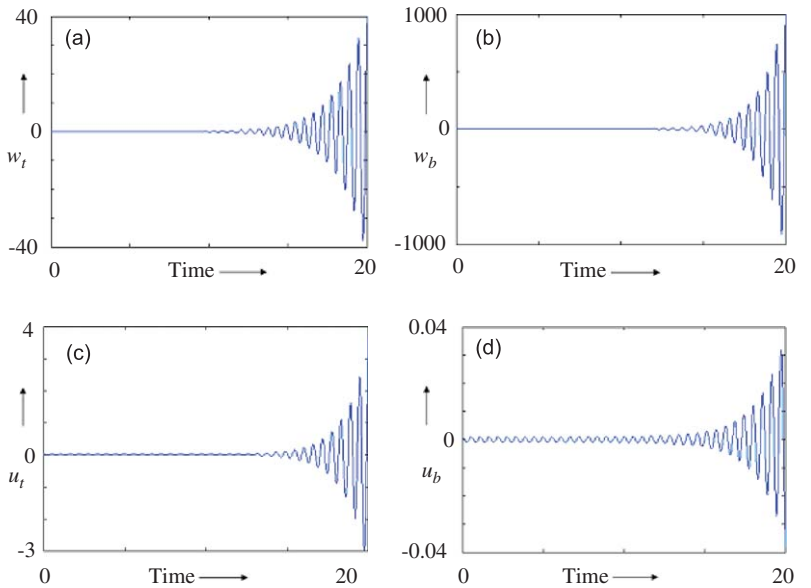

Fig. 3. Time response of soft-cored sandwich beam without MRE (at the point marked A in Fig. 2): (a) response of top skin in vertical direction (w_t), (b) response of bottom skin in vertical direction (w_b), (c) response of top skin in horizontal direction (u_t), and (d) response of bottom skin in horizontal direction (u_b).

taken as 0.1. As it has been shown by Deng and Gong [25] that the variation in core loss factor in MRE with magnetic field is negligible, here, for all conditions, core loss factor of 0.1 has been considered for both the MRE and non-MRE core materials.

In all the figures shown for instability regions, the curve with solid line represents the transition curves for the sandwich beam without MRE and the curve with dashed or dotted line represents the transition curves for a sandwich beam with a MRE patch placed at the middle of the core of the sandwich beam. It has been verified that using the equations given in Ref. [14] same instability regions have been obtained for the sandwich beam with only viscoelastic core (i.e., the system without MRE and magnetic field).

5.1. Simply supported beam

Considering the sandwich beam to be simply supported, Fig. 2 shows the principal parametric instability regions for the first three modes of sandwich beams with and without having a MRE patch. This is obtained by using the shape function given in Eq. (19) for a simply supported beam. For the beam with MRE, a magnetic field of 0.8 T has been considered.

It may clearly be observed that by using MRE patch one may alter the instability region. For example the point marked 'A' in Fig. 2 for principal parametric resonance of first mode is unstable for the sandwich beam without MRE as it is inside the unstable region. But the same point when considered for the sandwich beam with MRE is stable as it is outside the curves marked by the dashed line.

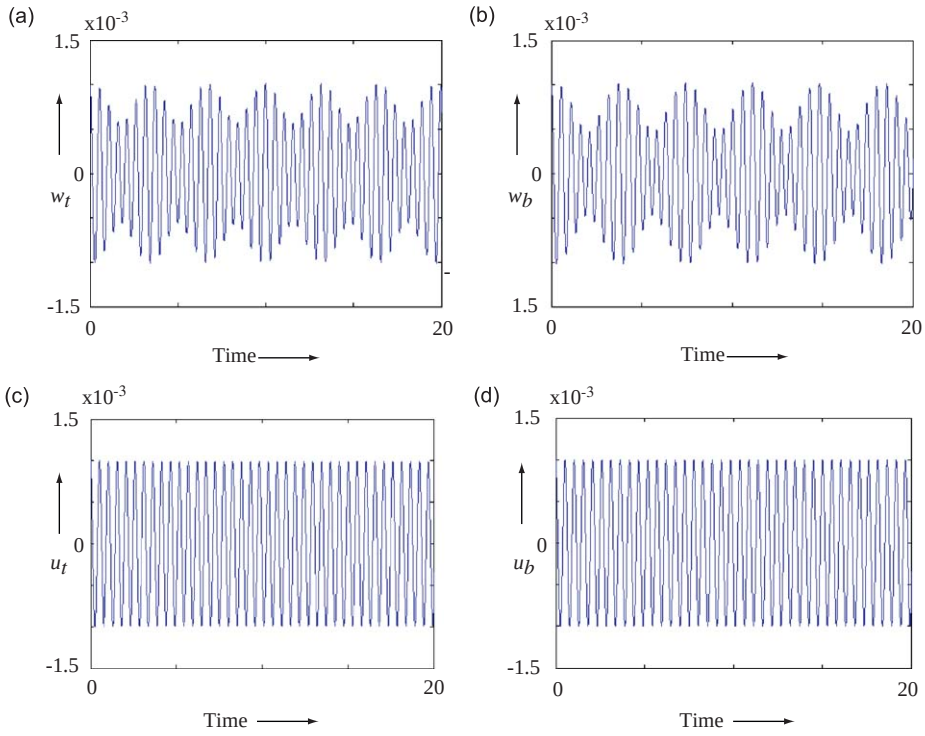

Fig. 4. Time response of soft-cored sandwich beam with MRE (at the point marked A in Fig. 2): (a) response of top skin in vertical direction (w_t), (b) response of bottom skin in vertical direction (w_b), (c) response of top skin in horizontal direction (u_t), and (d) response of bottom skin in horizontal direction (u_b).

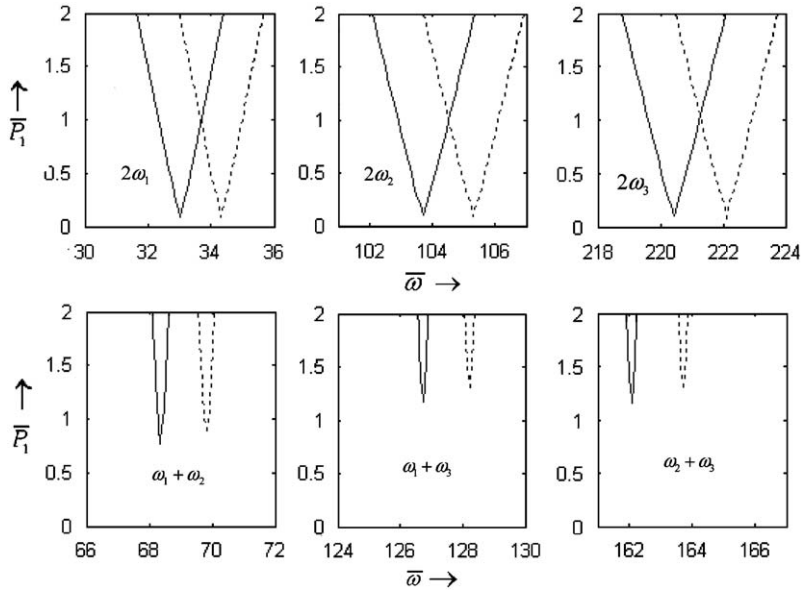

Fig. 5. Parametric instability regions of a clamped–pinned sandwich beam for the first three modes of principal and combination parametric resonances: ———, with soft-core and - - - - - - -, with MRE placed in the middle of soft-core.

To validate these results of instability regions, one may solve the temporal equation of motion Eq. (15) numerically to get the responses of the system. Figs. 3 and 4 show the time response for the point marked 'A' in Fig. 2. Figs. 3(a)–(d) clearly show that the time responses are unstable for the system without MRE, and Figs. 4(a)–(d) show that the system responses are stable when the beam is provided with a MRE patch in the middle. Hence, the unstable regions shown in the figures are in good agreement with those obtained by numerically solving the temporal equation of motion.

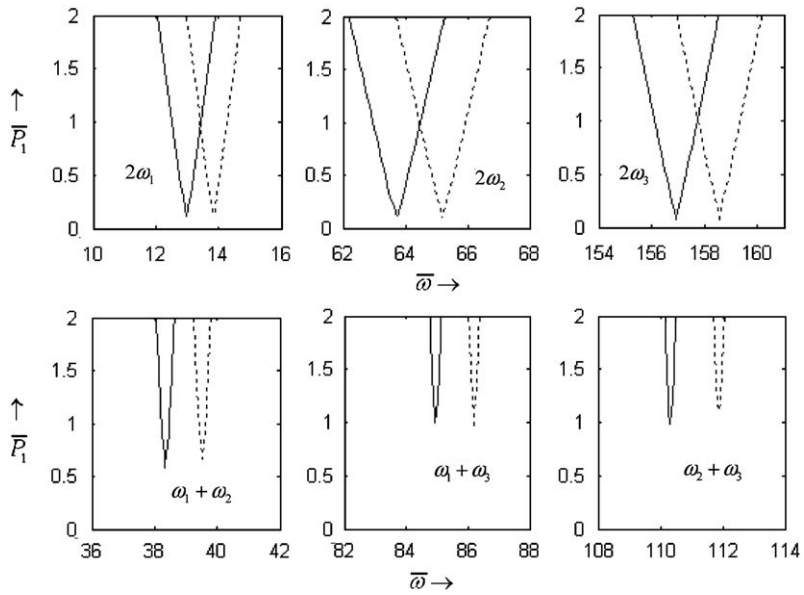

Fig. 6. Parametric instability regions of a clamped–guided sandwich beam for the first three modes of principal and combination parametric resonances: ———, with soft-core and - - - - - - -, with MRE placed in the middle of soft-core.

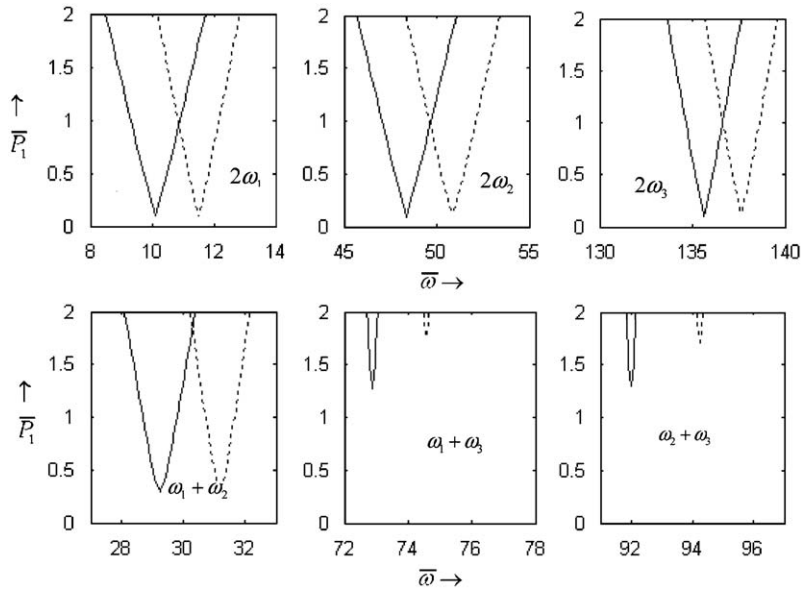

Fig. 7. Parametric instability regions of a clamped–free sandwich beam for the first three modes of principal and combination parametric resonances: ———, with soft-core and - - - - - - -, with MRE placed in the middle of soft-core.

From Fig. 2, it has been observed that the region of instability starts at a higher frequency while using a MRE patch at the middle portion of the core. This may be due to the fact that the properties of the MRE and non-MRE part of the core are considered to be the same, and due to the application of the magnetic filed, the stiffness of the sandwich structure increases which causes shifting of the instability region to a higher frequency. Hence, one may actively control the vibration of the sandwich structure by using MRE and applying magnetic field. It may be noted that the beam is observed to be stable in combination resonance of sum type and difference type.

5.2. Clamped–pinned beam

Using the shape function for the clamped–pinned beam as given in Eq. (20), the instability regions for the first three modes have been determined, and shown in Fig. 5. In this case the instability region starts at a higher frequency

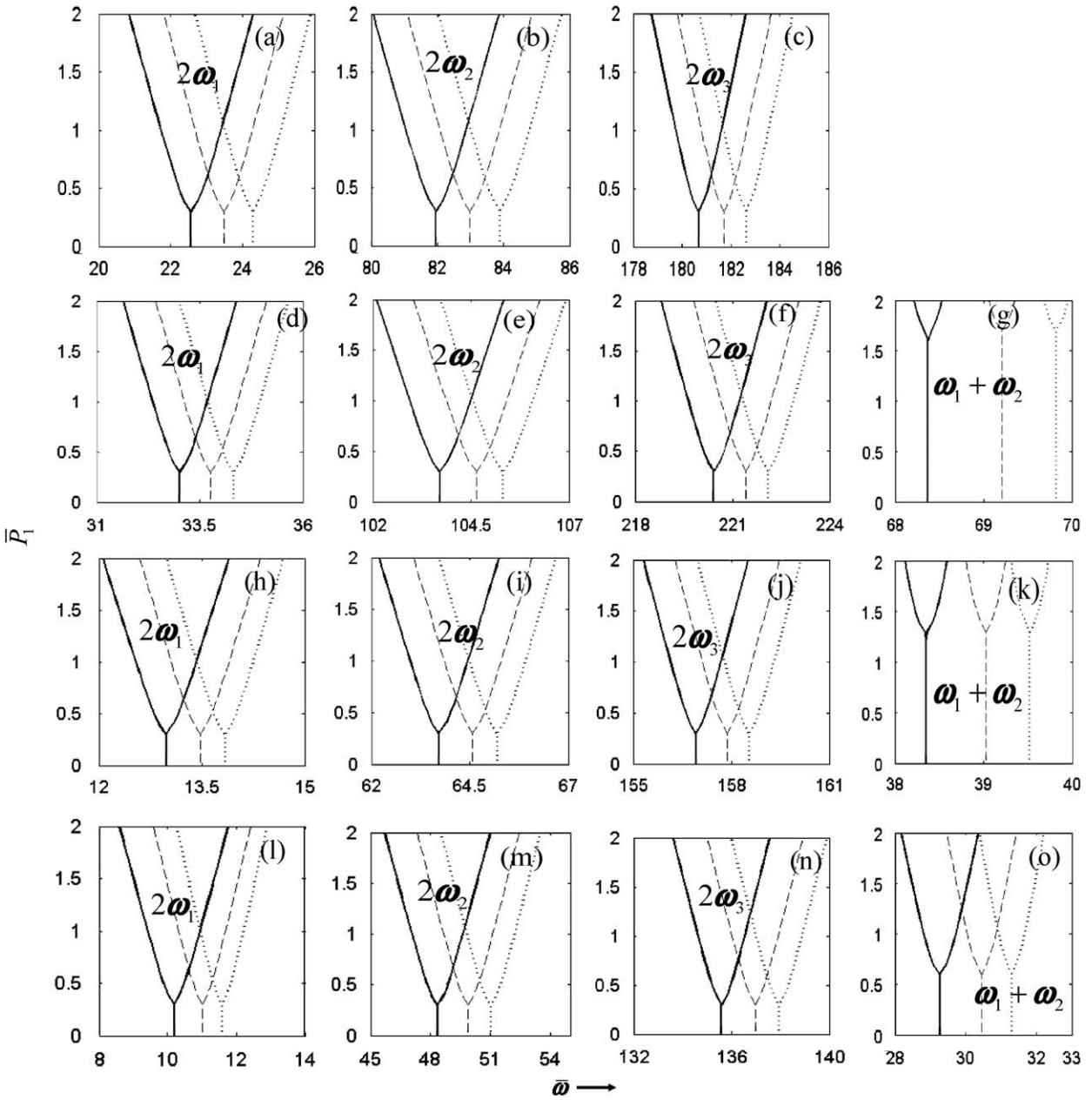

Fig. 8. Influence of magnetic field strength (B_0) on the parametric instability region for different boundary conditions: (a–c) simply supported, (d–g) clamped–pinned, (h–k) clamped–guided, and (l–o) clamped–free boundary conditions. Solid line (—) without MRE and without magnetic field, dashed line (- - - - - - -) with MRE $B_0 = 0.6$ T, and dotted line (……) $B_0 = 0.8$ T. $\mu_r = 10.0$.

than that of the simply supported beam, and similar to the simply supported case, here also, the instability region occurs at a higher frequency for a sandwich beam with a MRE patch. The beam is observed to be stable for combination resonance of difference type. The instability regions are smaller for combination resonance for sandwich beam with a MRE patch.

5.3. Clamped–guided beam

By taking into account the shape function given in Eq. (21) for the clamped–guided beam, the instability regions for the first three modes of vibration have been determined, and are shown in Fig. 6. Similar to the previous two cases, here

also, it can be observed that the instability regions occur at higher values of frequency in case of sandwich beam with MRE in comparison to that of a beam without MRE part. The beam is observed to be stable for combination resonance of difference type. As in this case, the natural frequencies of the system occur at lower frequencies as those of clamped–pinned beam, the instability regions have been found to occur at lower frequencies than those shown in Fig. 5.

5.4. Clamped–free beam

By using the shape function given in Eq. (22) for clamped–free beam, the instability regions for the clamped–free sandwich beams have been plotted in Fig. 7. Similar to the previous cases, here also, the effect of the addition of the MRE patch is to increase the stiffness, and so the shifting of the instability regions towards right. Also, it may be noted that in this boundary condition, the instability regions start at a lower frequency in comparison to the other three cases. In case of combination resonance of first and third mode, and second and third mode, the stability of the system improves significantly.

5.5. Variation of instability regions with magnetic field and relative permeability

Fig. 8 shows the instability regions of the sandwich beam for the above mentioned four boundary conditions with relative permeability of the skin materials μ_r equal to 10 and for three different values of magnetic field strength (viz., $B_0 = 0$, 0.6, and 0.8 T). Similar to the previous observations in Figs. 2–7, here also one may note that by using MRE patch and magnetic field one may change the instability region of the sandwich beam. With increase in magnetic filed strength, as the stiffness of the system increases, the instability region shifts toward right and hence, by suitably choosing the magnetic field strength one may actively control the vibration as explained in Fig. 2. From these figures, it may also be noted that while there is almost no change in the instability region in case of principal parametric resonance conditions, in combination resonance the system becomes more stable as the instability regions move upwards. Particularly, in the considered cases, the instability regions for combination resonances of higher modes ($\omega_2+\omega_3$, $\omega_3+\omega_1$) disappear indicating the system to be stable in these resonance conditions. Hence it has been observed that the use of skin materials with higher permeability improves the stability of the system particularly for combination resonance.

In Fig. 8 the instability regions for all four boundary conditions have been plotted to have a better comparison of the instability regions with different boundary conditions. Clearly among these four boundary conditions, the instability regions in case of clamped–free boundary condition occur at the lowest frequency and for clamped–pin beam it occurs at the highest frequency. This is due to the fact that for a given beam, the modal frequencies for clamped–free boundary condition is lowest and the corresponding modal frequencies for clamped–pin boundary is highest among the four boundaries considered in this work. Using these plots one may find the critical dynamic loading ($\bar{P}_{1cr}$) below which one may operate the system for the entire frequency range. This is marked by the vertical line in the instability plots in Fig. 8.

6. Conclusions

In this work, the governing equations of motion of a soft-cored symmetric sandwich beam with magnetorheological elastomer subjected to periodic axial end load has been derived using higher order theory. These equations have been reduced to that of a Mathieu–Hill's type of equations with complex coefficients which have been used to find the parametric instability regions by applying modified Hsu's method. The instability regions have been plotted for simply supported, clamped–guided, clamped–pinned, and clamped–free end conditions for the sandwich beam with and without MRE patch in the core. Also these regions are plotted for systems with principal parametric and combination parametric resonances of sum and difference types. The effects of skin permeability and the magnetic field strength on the instability regions have also been studied. The correctness of the instability regions has been verified by finding the time response from the temporal equation of motion and they have been found to be in good agreement.

In all the boundary conditions the regions of instability have been found to start at a higher frequency for the sandwich beam having an MRE patch in comparison to the sandwich beam without it. Also, it has been observed that, the stability of the systems improves significantly in case of combination resonance of sum type for the sandwich beam with MRE and with skin materials having higher relative permeability.

It has been understood that the vibration of a soft-cored sandwich beam can be actively controlled by suitably using magnetorheological elastomer patch and magnetic field. The developed equations will find a wide range of applications in studying the amount of attenuation of vibration one may obtain by using the magnetorheological elastomer in a sandwich beam when it is subjected to periodic axial loading.

Appendix A

$$(M_{11})_{ij} = (\bar{m}_t)\left(\int_0^1 w_{mi}w_{mj}\,d\bar{x}\right) + \bar{m}_c/3\left(\int_0^1 w_{mi}w_{mj}H_1\,d\bar{x}\right) + (\bar{m}_r/3)\left(\int_0^1 w_{mi}w_{mj}H_2\,d\bar{x}\right)$$
$$+ \{(\bar{m}_c/12)(d_t/L)^2\}\left(\int_0^1 w'_{mi}w'_{mj}H_1\,d\bar{x}\right) + \{(\bar{m}_r/12)(d_t/L)^2\}\left(\int_0^1 w'_{mi}w'_{mj}H_2\,d\bar{x}\right)$$
$$+ \{(\bar{m}_c/576)(d_t/c)(1+d_t/c)(c/L)^4(\xi_c/\phi_c)\}\left(\int_0^1 w''_{mi}w''_{mj}H_1\,d\bar{x}\right)$$
$$+ \{(\bar{m}_r/576)(d_t/c)(1+d_t/c)(c/L)^4(\xi_r/\phi_r)\}\left(\int_0^1 w''_{mi}w''_{mj}H_2\,d\bar{x}\right),$$

$$(M_{12})_{ij} = (\bar{m}_c/6)\left(\int_0^1 w_{mi}w_{qj}H_1\,d\bar{x}\right) + (\bar{m}_r/6)\left(\int_0^1 w_{mi}w_{qj}H_2\,d\bar{x}\right)$$
$$- \{(\bar{m}_c/24)(d_td_b/L^2)\}\left(\int_0^1 w'_{mi}w'_{qj}H_1\,d\bar{x}\right) + \{(\bar{m}_r/24)(d_td_b/L^2)\}\left(\int_0^1 w'_{mj}w'_{qi}H_2\,d\bar{x}\right)$$
$$+ \{(\bar{m}_c/576)(d_b/c)(1+d_t/c)(c/L)^4(\xi_c/\phi_c)\}\left(\int_0^1 w''_{mi}w''_{qj}H_1\,d\bar{x}\right)$$
$$+ \{(\bar{m}_r/576)(d_b/c)(1+d_t/c)(c/L)^4(\xi_r/\phi_r)\}\left(\int_0^1 w''_{mi}w''_{qj}H_2\,d\bar{x}\right),$$

$$(M_{13})_{ij} = -\{(\bar{m}_t)(1/48)(1+d_t/c)(c/L)^3(\xi_c/\phi_c)\}\left(\int_0^1 w''_{mi}u'_{rj}H_1\,d\bar{x}\right)$$
$$- \{(\bar{m}_t)(1/48)(1+d_t/c)(c/L)^3(\xi_r/\phi_r)\}\left(\int_0^1 w''_{mi}u'_{rj}H_2\,d\bar{x}\right)$$
$$+ \{(\bar{m}_c/288)(1+d_t/c)(c/L)^3(\xi_c/\phi_c)\}\left(\int_0^1 w''_{mi}u'_{rj}H_1\,d\bar{x}\right)$$
$$+ \{(\bar{m}_r/288)(1+d_t/c)(c/L)^3(\xi_r/\phi_r)\}\left(\int_0^1 w''_{mi}u'_{rj}H_2\,d\bar{x}\right)$$
$$- \{(\bar{m}_c/6)(d_t/L)\}\left(\int_0^1 w'_{mi}u_{rj}H_1\,d\bar{x}\right) - \{(\bar{m}_r/6)(d_t/L)\}\left(\int_0^1 w'_{mi}u_{rj}H_2\,d\bar{x}\right),$$

$$(M_{14})_{ij} = \{(1/48)(\bar{m}_b)(1+d_t/c)(c/L)^3(\xi_c/\phi_c)\}\left(\int_0^1 w''_{mi}u'_{sj}H_1\,d\bar{x}\right)$$
$$+ \{(1/48)(\bar{m}_b)(1+d_t/c)(c/L)^3(\xi_r/\phi_r)\}\left(\int_0^1 w''_{mi}u'_{sj}H_2\,d\bar{x}\right)$$
$$+ \{(1/48)(\bar{m}_c/6)(1+d_t/c)(c/L)^3(\xi_c/\phi_c)\}\left(\int_0^1 w''_{mi}u'_{sj}H_1\,d\bar{x}\right)$$
$$+ \{(1/48)(\bar{m}_r/6)(1+d_t/c)(c/L)^3(\xi_r/\phi_r)\}\left(\int_0^1 w''_{mi}u'_{sj}H_2\,d\bar{x}\right)$$
$$- \{(\bar{m}_c/12)(d_t/L)\}\left(\int_0^1 w'_{mi}u_{sj}H_1\,d\bar{x}\right) - \{(\bar{m}_r/12)(d_t/L)\}\left(\int_0^1 w'_{mi}u_{sj}H_2\,d\bar{x}\right),$$

$$(M_{21})_{ij} = (\bar{m}_c/6)\left(\int_0^1 w_{qi}w_{mj}H_1\,d\bar{x}\right) + (\bar{m}_r/6)\left(\int_0^1 w_{qi}w_{mj}H_2\,d\bar{x}\right)$$
$$- \{(\bar{m}_c/24)(d_td_b/L^2)\}\left(\int_0^1 w'_{qi}w'_{mj}H_1\,d\bar{x}\right) - \{(\bar{m}_r/24)(d_td_b/L^2)\}\left(\int_0^1 w'_{qi}w'_{mj}H_2\,d\bar{x}\right)$$

$$+\{(\bar{m}_c/576)(d_t/c)(1+d_b/c)(c/L)^4(\xi_c/\phi_c)\}\left(\int_0^1 w''_{qi}w''_{mj}H_1\,d\bar{x}\right)$$
$$+\{(\bar{m}_r/576)(d_t/c)(1+d_b/c)(c/L)^4(\xi_r/\phi_r)\}\left(\int_0^1 w''_{qi}w''_{mj}H_2\,d\bar{x}\right),$$

$$(M_{22})_{ij}=(\bar{m}_b)\left(\int_0^1 w_{qi}w_{qj}\,d\bar{x}\right)+(\bar{m}_c/3)\left(\int_0^1 w_{qi}w_{qj}H_1\,d\bar{x}\right)+(\bar{m}_r/3)\left(\int_0^1 w_{qi}w_{qj}H_2\,d\bar{x}\right)$$
$$+\{(\bar{m}_c/12)(d_t/L)^2\}\left(\int_0^1 w'_{qi}w'_{qj}H_1\,d\bar{x}\right)+\{(\bar{m}_r/12)(d_t/L)^2\}\left(\int_0^1 w'_{qi}w'_{qj}H_2\,d\bar{x}\right)$$
$$+\{(\bar{m}_c/576)(d_b/c)(1+d_b/c)(c/L)^4(\xi_c/\phi_c)\}\left(\int_0^1 w''_{qi}w''_{qj}H_1\,d\bar{x}\right)$$
$$+\{(\bar{m}_r/576)(d_b/c)(1+d_b/c)(c/L)^4(\xi_r/\phi_r)\}\left(\int_0^1 w''_{qi}w''_{qj}H_2\,d\bar{x}\right),$$

$$(M_{23})_{ij}=-\{(1/48)(\bar{m}_t)(1+d_b/c)(c/L)^3(\xi_c/\phi_c)\}\left(\int_0^1 w''_{qi}u'_{rj}H_1\,d\bar{x}\right)$$
$$-\{(1/48)(\bar{m}_t)(1+d_b/c)(c/L)^3(\xi_r/\phi_r)\}\left(\int_0^1 w''_{qi}u'_{rj}H_2\,d\bar{x}\right)$$
$$-\{(1/48)(\bar{m}_c/6)(1+d_b/c)(c/L)^3(\xi_c/\phi_c)\}\left(\int_0^1 w''_{qi}u'_{rj}H_1\,d\bar{x}\right)$$
$$-\{(1/48)(\bar{m}_r/6)(1+d_b/c)(c/L)^3(\xi_r/\phi_r)\}\left(\int_0^1 w''_{qi}u'_{rj}H_2\,d\bar{x}\right)$$
$$+\{(m_c/12)(d_b/L)\}\left(\int_0^1 w'_{qi}u_{rj}H_1\,d\bar{x}\right)+\{(m_r/12)(d_b/L)\}\left(\int_0^1 w'_{qi}u_{rj}H_2\,d\bar{x}\right),$$

$$(M_{24})_{ij}=\{(1/48)(\bar{m}_b)(1+d_b/c)(c/L)^3(\xi_c/\phi_c)\}\left(\int_0^1 w''_{qi}u'_{sj}H_1\,d\bar{x}\right)$$
$$+\{(1/48)(\bar{m}_b)(1+d_b/c)(c/L)^3(\xi_r/\phi_r)\}\left(\int_0^1 w''_{qi}u'_{sj}H_2\,d\bar{x}\right)$$
$$+\{(1/48)(\bar{m}_c/6)(1+d_b/c)(c/L)^3(\xi_c/\phi_c)\}\left(\int_0^1 w''_{qi}u'_{sj}H_1\,d\bar{x}\right)$$
$$+\{(1/48)(\bar{m}_r/6)(1+d_b/c)(c/L)^3(\xi_r/\phi_r)\}\left(\int_0^1 w''_{qi}u'_{sj}H_2\,d\bar{x}\right)$$
$$+(m_c/6)(d_b/L)\left(\int_0^1 w'_{qi}u_{sj}H_1\,d\bar{x}\right)+(m_r/6)(d_b/L)\left(\int_0^1 w'_{qi}u_{sj}H_2\,d\bar{x}\right),$$

$$(M_{31})_{ij}=-\{(m_c/288)(d_t/c)(c/L)^3(\xi_c/\phi_c)\}\left(\int_0^1 u''_{ri}w'_{mj}H_1\,d\bar{x}\right)$$
$$-\{(m_r/288)(d_t/c)(c/L)^3(\xi_r/\phi_r)\}\left(\int_0^1 u''_{ri}w'_{mj}H_2\,d\bar{x}\right)$$
$$-\{(\bar{m}_c/6)(d_t/L)\}\left(\int_0^1 u'_{ri}w_{mj}H_1\,d\bar{x}\right)-\{(\bar{m}_r/6)(d_t/L)\}\left(\int_0^1 u'_{ri}w_{mj}H_2\,d\bar{x}\right),$$

$$(M_{32})_{ij}=\{(\bar{m}_c/12)(d_b/L)\}\left(\int_0^1 u'_{ri}w_{qj}H_1\,d\bar{x}\right)+\{(\bar{m}_r/12)(d_b/L)\}\left(\int_0^1 u'_{ri}w_{qj}H_2\,d\bar{x}\right)$$
$$-\{(\bar{m}_c/288)(d_b/c)(c/L)^3(\xi_c/\phi_c)\}\left(\int_0^1 u''_{ri}w'_{qj}H_1\,d\bar{x}\right)$$
$$-\{(\bar{m}_r/288)(d_b/c)(c/L)^3(\xi_r/\phi_r)\}\left(\int_0^1 u''_{ri}w'_{qj}H_2\,d\bar{x}\right),$$

$$
\begin{aligned}
(M_{33})_{ij} = & -\{(1/24)(\bar{m}_t)(c/L)^2(\xi_c/\phi_c)\}\left(\int_0^1 u'_{ri}u'_{rj}H_1\,\mathrm{d}\bar{x}\right)\\
& -\{(1/24)(\bar{m}_t)(c/L)^2(\xi_r/\phi_r)\}\left(\int_0^1 u'_{ri}u'_{rj}H_2\,\mathrm{d}\bar{x}\right)\\
& -\{(1/24)(\bar{m}_c/6)(c/L)^2(\xi_c/\phi_c)\}\left(\int_0^1 u'_{ri}u'_{rj}H_1\,\mathrm{d}\bar{x}\right)\\
& -\{(1/24)(\bar{m}_r/6)(c/L)^2(\xi_r/\phi_r)\}\left(\int_0^1 u'_{ri}u'_{rj}H_2\,\mathrm{d}\bar{x}\right)\\
& -(\bar{m}_t)\left(\int_0^L u_{ri}u_{rj}\,\mathrm{d}\bar{x}\right)-(\bar{m}_c/3)\left(\int_0^1 u_{ri}u_{rj}H_1\,\mathrm{d}\bar{x}\right)-(\bar{m}_c/3)\left(\int_0^1 u_{ri}u_{rj}H_2\,\mathrm{d}\bar{x}\right),
\end{aligned}
$$

$$
\begin{aligned}
(M_{34})_{ij} = & -(\bar{m}_c/6)\left(\int_0^1 u_{ri}u_{sj}H_1\,\mathrm{d}\bar{x}\right)-(\bar{m}_r/6)\left(\int_0^1 u_{ri}u_{sj}H_2\,\mathrm{d}\bar{x}\right)\\
& +\{(\bar{m}_b/24)(c/L)^2(\xi_c/\phi_c)\}\left(\int_0^1 u'_{ri}u'_{sj}H_1\,\mathrm{d}\bar{x}\right)+\{(\bar{m}_b/24)(c/L)^2(\xi_r/\phi_r)\}\left(\int_0^1 u'_{ri}u'_{sj}H_2\,\mathrm{d}\bar{x}\right)\\
& +\{(\bar{m}_c/144)(c/L)^2(\xi_c/\phi_c)\}\left(\int_0^1 u'_{ri}u'_{sj}H_1\,\mathrm{d}\bar{x}\right)+\{(\bar{m}_c/144)(c/L)^2(\xi_r/\phi_r)\}\left(\int_0^1 u'_{ri}u'_{sj}H_2\,\mathrm{d}\bar{x}\right),
\end{aligned}
$$

$$
\begin{aligned}
(M_{41})_{ij} = & -\{(\bar{m}_c/12)(d_t/L)\}\left(\int_0^1 u'_{si}w_{mj}H_1\,\mathrm{d}\bar{x}\right)-\{(\bar{m}_r/12)(d_t/L)\}\left(\int_0^1 u'_{si}w_{mj}H_2\,\mathrm{d}\bar{x}\right)\\
& +\{(\bar{m}_c/288)(d_t/c)(c/L)^3(\xi_c/\phi_c)\}\left(\int_0^1 u''_{si}w'_{mj}H_1\,\mathrm{d}\bar{x}\right)\\
& +\{(\bar{m}_r/288)(d_t/c)(c/L)^3(\xi_r/\phi_r)\}\left(\int_0^1 u''_{si}w'_{mj}H_2\,\mathrm{d}\bar{x}\right),
\end{aligned}
$$

$$
\begin{aligned}
(M_{42})_{ij} = & \{(\bar{m}_c/6)(d_b/L)\}\left(\int_0^1 u'_{si}w_{qj}H_1\,\mathrm{d}\bar{x}\right)+\{(\bar{m}_r/6)(d_b/L)\}\left(\int_0^1 u'_{si}w_{qj}H_2\,\mathrm{d}\bar{x}\right)\\
& +\{(\bar{m}_c/288)(d_b/c)(c/L)^3(\xi_c/\phi_c)\}\left(\int_0^1 u''_{si}w'_{qj}H_1\,\mathrm{d}\bar{x}\right)\\
& +\{(\bar{m}_r/288)(d_b/c)(c/L)^3(\xi_r/\phi_r)\}\left(\int_0^1 u''_{si}w'_{qj}H_2\,\mathrm{d}\bar{x}\right),
\end{aligned}
$$

$$
\begin{aligned}
(M_{43})_{ij} = & -(\bar{m}_c/6)\left(\int_0^1 u_{si}u_{rj}H_1\,\mathrm{d}\bar{x}\right)-(\bar{m}_r/6)\left(\int_0^1 u_{si}u_{rj}H_2\,\mathrm{d}\bar{x}\right)\\
& +\{(\bar{m}_t/24)(c/L)^2(\xi_c/\phi_c)\}\left(\int_0^1 u'_{si}u'_{rj}H_1\,\mathrm{d}\bar{x}\right)+\{(\bar{m}_t/24)(c/L)^2(\xi_r/\phi_r)\}\left(\int_0^1 u'_{si}u'_{rj}H_2\,\mathrm{d}\bar{x}\right)\\
& +\{(\bar{m}_c/144)(c/L)^2(\xi_c/\phi_c)\}\left(\int_0^1 u'_{si}u'_{rj}H_1\,\mathrm{d}\bar{x}\right)+\{(\bar{m}_r/144)(c/L)^2(\xi_r/\phi_r)\}\left(\int_0^1 u'_{si}u'_{rj}H_2\,\mathrm{d}\bar{x}\right),
\end{aligned}
$$

$$
\begin{aligned}
(M_{44})_{ij} = & -(\bar{m}_b)\left(\int_0^1 u_{si}u_{sj}\,\mathrm{d}\bar{x}\right)-(\bar{m}_c/3)\left(\int_0^1 u_{si}u_{sj}H_1\,\mathrm{d}\bar{x}\right)-(\bar{m}_r/3)\left(\int_0^1 u_{si}u_{sj}H_2\,\mathrm{d}\bar{x}\right)\\
& -\{(\bar{m}_b/24)(c/L)^2(\xi_c/\phi_c)\}\left(\int_0^1 u'_{si}u'_{sj}H_1\,\mathrm{d}\bar{x}\right)-\{(\bar{m}_b/24)(c/L)^2(\xi_r/\phi_r)\}\left(\int_0^1 u'_{si}u'_{sj}H_2\,\mathrm{d}\bar{x}\right)\\
& -\{(\bar{m}_c/144)(c/L)^2(\xi_c/\phi_c)\}\left(\int_0^1 u'_{si}u'_{sj}H_1\,\mathrm{d}\bar{x}\right)-\{(\bar{m}_r/144)(c/L)^2(\xi_r/\phi_r)\}\left(\int_0^1 u'_{si}u'_{sj}H_2\,\mathrm{d}\bar{x}\right),
\end{aligned}
$$

$$(K_{11})_{ij} = \{(\xi_c/4)(1+d_t/c)^2\}\left(\int_0^1 w'_{mi}w'_{mj}H_1\,d\bar{x}\right) + \{(\xi_c/4)(1+d_t/c)^2\}\left(\int_0^1 w'_{mi}w'_{mj}H_2\,d\bar{x}\right) + \{(\phi_t/12)(d_t/L)^2\}\left(\int_0^1 w''_{mi}w'_{mj}\,d\bar{x}\right) + \{\phi_c(L/c)^2\}\left(\int_0^1 w_{mi}w_{mj}H_1\,d\bar{x}\right) + \{\phi_r(L/c)^2\}\left(\int_0^1 w_{mi}w_{mj}H_2\,d\bar{x}\right),$$

$$(K_{12})_{ij} = -\{\phi_c(L/c)^2\}\left(\int_0^1 w_{mi}w_{qj}H_1\,d\bar{x}\right) + \{(\xi_c/4)(1+d_t/c)(1+d_b/c)\}\left(\int_0^1 w'_{mi}w'_{qj}H_1\,d\bar{x}\right) + \{(\xi_r/4)(1+d_t/c)(1+d_b/c)\}\left(\int_0^1 w'_{mi}w'_{qj}H_2\,d\bar{x}\right) - \{\phi_r(L/c)^2\}\left(\int_0^1 w_{mi}w_{qj}H_2\,d\bar{x}\right),$$

$$(K_{13})_{ij} = -\{(\xi_c/2)(L/c)(1+d_t/c)\}\left(\int_0^1 w'_{mi}u_{rj}H_1\,d\bar{x}\right) - \{(\xi_r/2)(L/c)(1+d_t/c)\}\left(\int_0^1 w'_{mi}u_{rj}H_2\,d\bar{x}\right) - \{(\phi_t/48)(c/L)^3(1+d_t/c)(\xi_c/\phi_c)\}\left(\int_0^1 w'''_{mi}u''_{rj}H_1\,d\bar{x}\right) - \{(\phi_t/48)(c/L)^3(1+d_t/c)(\xi_r/\phi_r)\}\left(\int_0^1 w'''_{mi}u''_{rj}H_2\,d\bar{x}\right),$$

$$(K_{14})_{ij} = \{(\xi_c/2)(L/c)(1+d_t/c)\}\left(\int_0^1 w'_{mi}u_{sj}H_1\,d\bar{x}\right) + \{(\xi_r/2)(L/c)(1+d_t/c)\}\left(\int_0^1 w'_{mi}u_{sj}H_2\,d\bar{x}\right) + \{(\phi_b/48)(c/L)^3(1+d_t/c)(\xi_c/\phi_c)\}\left(\int_0^1 w'''_{mi}u''_{sj}H_1\,d\bar{x}\right) + \{(\phi_b/48)(c/L)^3(1+d_t/c)(\xi_r/\phi_r)\}\left(\int_0^1 w'''_{mi}u''_{sj}H_2\,d\bar{x}\right),$$

$$(K_{21})_{ij} = -\{\phi_c(L/c)^2\}\left(\int_0^1 w_{qi}w_{mj}\,d\bar{x}\right) + \{(\xi_c/4)(1+d_t/c)(1+d_b/c)\}\left(\int_0^1 w'_{qi}w'_{mj}H_1\,d\bar{x}\right) + \{(\xi_r/4)(1+d_t/c)(1+d_b/c)\}\left(\int_0^1 w'_{qi}w'_{mj}H_2\,d\bar{x}\right),$$

$$(K_{22})_{ij} = \{(\xi_c/4)(1+d_b/c)^2\}\left(\int_0^1 w'_{qi}w'_{qj}H_1\,d\bar{x}\right) + \{(\xi_r/4)(1+d_b/c)^2\}\left(\int_0^1 w'_{qi}w'_{qj}H_2\,d\bar{x}\right) + \{(\phi_b/12)(d_b/L)^2\}\left(\int_0^1 w''_{qi}w''_{qj}\,d\bar{x}\right),$$

$$(K_{23})_{ij} = \{(-\xi_c/2)(L/c)(1+d_b/c)\}\left(\int_0^1 w'_{qi}u_{rj}H_1\,d\bar{x}\right) + \{(-\xi_r/2)(L/c)(1+d_b/c)\}\left(\int_0^1 w'_{qi}u_{rj}H_2\,d\bar{x}\right) - \{(\phi_t/48)(c/L)^3(1+d_b/c)(\xi_c/\phi_c)\}\left(\int_0^1 w'''_{qi}u''_{rj}H_1\,d\bar{x}\right) - \{(\phi_t/48)(c/L)^3(1+d_b/c)(\xi_r/\phi_r)\}\left(\int_0^1 w'''_{qi}u''_{rj}H_2\,d\bar{x}\right),$$

$$(K_{24})_{ij} = \{(\xi_c/2)(L/c)(1+d_b/c)\}\left(\int_0^1 w'_{qi}u_{sj}H_1\,d\bar{x}\right) + \{(\xi_r/2)(L/c)(1+d_b/c)\}\left(\int_0^1 w'_{qi}u_{sj}H_2\,d\bar{x}\right) + \{(\phi_b/48)(c/L)^3(1+d_b/c)(\xi_c/\phi_c)\}\left(\int_0^1 w'''_{qi}u''_{sj}H_1\,d\bar{x}\right) + \{(\phi_b/48)(c/L)^3(1+d_b/c)(\xi_r/\phi_r)\}\left(\int_0^1 w'''_{qi}u''_{sj}H_2\,d\bar{x}\right),$$

$$(K_{31})_{ij} = \{(-\xi_c/2)(L/c)(1+d_t/c)\}\left(\int_0^1 u'_{ri} w_{mj} H_1 \,\mathrm{d}\bar{x}\right) + \{(-\xi_r/2)(L/c)(1+d_t/c)\}\left(\int_0^1 u'_{ri} w_{mj} H_2 \,\mathrm{d}\bar{x}\right),$$

$$(K_{32})_{ij} = \{(-\xi_c/2)(L/c)(1+d_b/c)\}\left(\int_0^1 u'_{ri} w_{qj} H_1 \,\mathrm{d}\bar{x}\right) + \{(-\xi_r/2)(L/c)(1+d_b/c)\}\left(\int_0^1 u'_{ri} w_{qj} H_2 \,\mathrm{d}\bar{x}\right),$$

$$\begin{aligned}(K_{33})_{ij} = {} & (-\phi_t)\left(\int_0^1 u'_{ri} u'_{rj} \,\mathrm{d}\bar{x}\right) - \{(L/c)^2 \xi_c\}\left(\int_0^1 u_{ri} u_{rj} H_1 \,\mathrm{d}\bar{x}\right) - \{(L/c)^2 \xi_r\}\left(\int_0^1 u_{ri} u_{rj} H_2 \,\mathrm{d}\bar{x}\right) \\ & - \{(\phi_t/24)(c/L)^2(\xi_c/\phi_c)\}\left(\int_0^L u''_{ri} u''_{rj} H_1 \,\mathrm{d}\bar{x}\right) - \{(\phi_t/24)(c/L)^2(\xi_r/\phi_r)\}\left(\int_0^L u''_{ri} u''_{rj} H_2 \,\mathrm{d}\bar{x}\right),\end{aligned}$$

$$\begin{aligned}(K_{34})_{ij} = {} & \{(L/c)^2 \xi_c\}\left(\int_0^1 u_{ri} u_{sj} H_1 \,\mathrm{d}\bar{x}\right) + \{(L/c)^2 \xi_r\}\left(\int_0^1 u_{ri} u_{sj} H_2 \,\mathrm{d}\bar{x}\right) \\ & + \{(\phi_b/24)(c/L)^2(\xi_c/\phi_c)\}\left(\int_0^1 u''_{ri} u''_{sj} H_1 \,\mathrm{d}\bar{x}\right) + \{(\phi_b/24)(c/L)^2(\xi_r/\phi_r)\}\left(\int_0^1 u''_{ri} u''_{sj} H_2 \,\mathrm{d}\bar{x}\right),\end{aligned}$$

$$(K_{41})_{ij} = \{(\xi_c/2)(L/c)(1+d_t/c)\}\left(\int_0^1 u'_{si} w_{mj} H_1 \,\mathrm{d}\bar{x}\right) + \{(\xi_r/2)(L/c)(1+d_t/c)\}\left(\int_0^1 u'_{si} w_{mj} H_2 \,\mathrm{d}\bar{x}\right),$$

$$(K_{42})_{ij} = \{(\xi_c/2)(L/c)(1+d_b/c)\}\left(\int_0^1 u'_{si} w_{qj} H_1 \,\mathrm{d}\bar{x}\right) + \{(\xi_r/2)(L/c)(1+d_b/c)\}\left(\int_0^1 u'_{si} w_{qj} H_2 \,\mathrm{d}\bar{x}\right),$$

$$\begin{aligned}(K_{43})_{ij} = {} & \{(L/c)^2 \xi_c\}\left(\int_0^1 u_{si} u_{rj} H_1 \,\mathrm{d}\bar{x}\right) + \{(L/c)^2 \xi_r\}\left(\int_0^1 u_{si} u_{rj} H_2 \,\mathrm{d}\bar{x}\right) \\ & + \{(\phi_t/24)(c/L)^2(\xi_c/\phi_c)\}\left(\int_0^1 u''_{si} u''_{rj} H_1 \,\mathrm{d}\bar{x}\right) + \{(\phi_t/24)(c/L)^2(\xi_r/\phi_r)\}\left(\int_0^1 u''_{si} u''_{rj} H_2 \,\mathrm{d}\bar{x}\right),\end{aligned}$$

$$\begin{aligned}(K_{44})_{ij} = {} & (-\phi_b)\left(\int_0^1 u'_{si} u'_{sj} \,\mathrm{d}\bar{x}\right) - \{(L/c)^2 \xi_c\}\left(\int_0^1 u_{si} u_{sj} H_1 \,\mathrm{d}\bar{x}\right) - \{(L/c)^2 \xi_r\}\left(\int_0^1 u_{si} u_{sj} H_2 \,\mathrm{d}\bar{x}\right) \\ & - \{(\phi_b/24)(c/L)^2(\xi_c/\phi_c)\}\left(\int_0^1 u''_{si} u''_{sj} H_1 \,\mathrm{d}\bar{x}\right) - \{(\phi_b/24)(c/L)^2(\xi_r/\phi_r)\}\left(\int_0^1 u''_{si} u''_{sj} H_2 \,\mathrm{d}\bar{x}\right),\end{aligned}$$

$$[F_{11}]_{ij} = \int_0^1 w'_{qi} w'_{qj} \,\mathrm{d}\bar{x},$$

$$[F_{22}]_{ij} = \int_0^1 w'_{mi} w'_{mj} \,\mathrm{d}\bar{x},$$

$$\begin{aligned}(H_{11})_{ij} = {} & -B_0^2 b d_t^2 L/(2\pi\mu_0 E)\left(\int_0^1 (\ln(\bar{x}/(1-\bar{x})))_{,\bar{x}} w'_{mi} w'_{mj} \,\mathrm{d}\bar{x}\right) \\ & + B_0^2 b d_t^2 L/(2\pi\mu_0 E)\left(\int_0^1 \ln(\bar{x}/(1-\bar{x})) w''_{mi} w'_{mj} \,\mathrm{d}\bar{x}\right) \\ & + B_0^2 b d_t L^2/(\mu_0 E)\left(\int_0^1 w'_{mi} w'_{mj} \,\mathrm{d}\bar{x}\right) + B_0^2 b d_t^3/(12 E \mu_{et})\left(\int_0^1 w''_{mi} w''_{mj} \,\mathrm{d}\bar{x}\right),\end{aligned}$$

$$(H_{12})_{ij} = 0,$$

$$\begin{aligned}(H_{13})_{ij} = {} & B_0^2 b d_t L^2 \pi/(2\mu_0 E)\left(\int_0^1 (1/(\ln(\bar{x}/(1-\bar{x}))))_{,\bar{x}} w'_{mi} u_{rj} \,\mathrm{d}\bar{x}\right) \\ & + B_0^2 b d_t L^2/(2\mu_0 E)\left(\int_0^1 \pi/(\ln(\bar{x}/(1-\bar{x}))) w'_{mi} u'_{rj} \,\mathrm{d}\bar{x}\right) \\ & + B_0^2 b d_t c^3 G_c/(48 E_c E L \mu_{et})(1+d_t/c)\left(\int_0^1 w'''_{mi} u''_{rj} \,\mathrm{d}\bar{x}\right),\end{aligned}$$

$$(H_{14})_{ij} = -B_0^2 b d_b c^3 G_c/(48 E_c E L \mu_{eb})(1 + d_t/c)\left(\int_0^1 w'''_{mi} u''_{sj}\,\mathrm{d}\bar{x}\right),$$

$$(H_{21})_{ij} = 0,$$

$$\begin{aligned}(H_{22})_{ij} = &-B_0^2 b d_b^2 L/(2\pi\mu_0 E)\left(\int_0^1 (\ln(\bar{x}/(1-\bar{x})))_{,\bar{x}} w'_{qi} w'_{qj}\,\mathrm{d}\bar{x}\right)\\ &+ B_0^2 b d_t^2 L/(2\pi\mu_0 E)\left(\int_0^1 \ln(\bar{x}/(1-\bar{x})) w''_{qi} w''_{qj}\,\mathrm{d}\bar{x}\right)\\ &+ B_0^2 b d_b L^2/(\mu_0 E)\left(\int_0^1 w'_{qi} w'_{qj}\,\mathrm{d}\bar{x}\right) + B_0^2 b d_b^3/(12 E \mu_{et})\left(\int_0^1 w''_{qi} w''_{qj}\,\mathrm{d}\bar{x}\right),\end{aligned}$$

$$(H_{23})_{ij} = B_0^2 b d_t c^3 G_c/(48 E_c E L \mu_{et})(1 + d_b/c)\left(\int_0^1 w'''_{qi} u''_{rj}\,\mathrm{d}\bar{x}\right),$$

$$\begin{aligned}(H_{24})_{ij} = &B_0^2 b d_b L^2 \pi/(2\mu_0 E)\left(\int_0^1 (1/(\ln(\bar{x}/(1-\bar{x}))))_{,\bar{x}} w'_{qi} u_{sj}\,\mathrm{d}\bar{x}\right)\\ &+ B_0^2 b d_b L^2/(2\mu_0 E)\left(\int_0^1 \pi/(\ln(\bar{x}/(1-\bar{x}))) w'_{qi} u'_{sj}\,\mathrm{d}\bar{x}\right)\\ &- B_0^2 b d_b c^3 G_c/(48 E_c E L \mu_{eb})(1 + d_b/c)\left(\int_0^1 w'''_{qi} u''_{sj}\,\mathrm{d}\bar{x}\right),\end{aligned}$$

$$(H_{31})_{ij} = 0,$$

$$(H_{32})_{ij} = 0,$$

$$(H_{33})_{ij} = B_0^2 b d_t L^2/(\mu_{et} E)\left(\int_0^1 u'_{ri} u'_{rj}\,\mathrm{d}\bar{x}\right) + B_0^2 b d_t c^2 G_c/(24\mu_{et} E E_c)\left(\int_0^1 u''_{ri} u''_{rj}\,\mathrm{d}\bar{x}\right),$$

$$(H_{34})_{ij} = -B_0^2 b d_b c^2 G_c/(24\mu_{eb} E E_c)\left(\int_0^1 u''_{ri} u''_{sj}\,\mathrm{d}\bar{x}\right),$$

$$(H_{41})_{ij} = 0,$$

$$(H_{42})_{ij} = 0,$$

$$(H_{43})_{ij} = -B_0^2 b d_t c^2 G_c/(24\mu_{et} E E_c)\left(\int_0^1 u''_{si} u''_{rj}\,\mathrm{d}\bar{x}\right),$$

$$(H_{44})_{ij} = B_0^2 b d_b L^2/(\mu_{eb} E)\left(\int_0^1 u'_{si} u'_{sj}\,\mathrm{d}\bar{x}\right) + B_0^2 b d_b c^2 G_c/(24\mu_{eb} E E_c)\left(\int_0^1 u''_{si} u''_{sj}\,\mathrm{d}\bar{x}\right),$$

where t is for top layer and b is for bottom layer. In the above relations, $w'_{(\,)i} = \partial w_{(\,)i}/\partial\bar{x}$, and the submatrices which are not covered by the above elements should be treated as null.

References

[1] R.A. Ditaranto, Theory of vibratory bending for elastic and viscoelastic layered finite-length beams, *Journal of Applied Mechanics* 32 (1965) 881–886.
[2] N.T. Asnani, B.C. Nakra, Vibration analysis of multilayered beams with alternate elastic and viscoelastic layers, *Journal of Institution of Engineers (India)—Mechanical Engineering Division* 50 (1970) 187–193.
[3] B.C. Nakra, Structural dynamic modification using additive damping, *Sadhana* 25 (3) (2000) 277–289.
[4] Y. Frostig, M. Baruch, Bending of sandwich beams with transversely flexible core, *American Institute of Aeronautics and Astronautics Journal* 27 (1990) 523–531.
[5] Y. Frostig, M. Baruch, Free vibrations of sandwich beams with a transversely flexible core: a higher order approach, *Journal of Sound and Vibration* 176 (2) (1994) 195–208.
[6] Y. Frostig, Buckling of sandwich panels with flexible core—high order theory, *International Journal of Solids and Structures* 35 (3–4) (1998) 183–204.
[7] A.H. Nayfeh, D.T. Mook, *Non-linear Oscillations*, Wiley-Interscience, New York, 1979.
[8] M.P. Cartmell, *Introduction to Linear parametric and Non-linear Vibrations*, Chapman & Hall, London, 1990.
[9] H. Saito, K. Otomi, Parametric response of viscoelastically supported beams, *Journal of Sound and Vibration* 63 (1979) 169–178.
[10] C.S. Hsu, On the parametric excitation of a dynamic system having multiple degrees of freedom, *ASME Journal of Applied Mechanics* 30 (1963) 367–372.
[11] R.C. Kar, T. Sujata, Dynamic stability of a tapered symmetric sandwich beam, *Computers & Structures* 40 (1991) 1441–1449.

[12] K. Ray, R.C. Kar, Parametric instability of a sandwich beam with various boundary conditions, *Computers & Structures* 55 (1995) 857–870.
[13] K. Ray, R.C. Kar, Parametric instability of multi-layered sandwich beams, *Journal of Sound and Vibration* 193 (1996) 631–644.
[14] S.K. Dwivedy, K.C. Sahu, Sk. Babu, Parametric instability regions of three layered soft-cored sandwich beam using higher order theory, *Journal of Sound and Vibration* 304 (2007) 326–344.
[15] T. Shiga, A. Okada, T. Kurauchi, Magnetroviscoelastic behavior of composite gels, *Journal of Applied Polymer Science* 58 (1995) 787–792.
[16] M.R. Jolly, J.D. Carlson, B.C. Munoz, A. Bullions, The magneto viscoelastic response of elastomer composites consisting of ferrous particles embedded in a polymer matrix, *Journal of Intelligent Material Systems and Structures* 7 (1996) 613–622.
[17] J.D. Carlson, M.R. Jolly, MR fluid, foam and elastomer devices, *Mechatronics* 10 (2000) 555–569.
[18] L.C. Davis, Model of magnetorheological elastomers, *Journal of Applied Physics* 85 (1999) 3348–3351.
[19] G.Y. Zhou, Complex shear modulus of a magnetorheological elastomer, *Smart Materials and Structures* 13 (2004) 1203–1210.
[20] G.Y. Zhou, Q. Wang, Magnetorheological elastomer-based smart sandwich beam with nonconductive skins, *Smart Materials and Structures* 14 (2005) 1001–1009.
[21] G.Y. Zhou, Q. Wang, Use of magnetorheological elastomer in adaptive sandwich beam with conductive skins—part I: magnetoelastic loads in conductive skins, *International Journal of Solids and Structures* 43 (2006) 5386–5402.
[22] G.Y. Zhou, Q. Wang, Use of magnetorheological elastomer in adaptive sandwich beam with conductive skins—part II: dynamic property, *International Journal of Solids and Structures* 43 (2006) 5403–5420.
[23] L. Chen, X.L. Gong, W.Q. Jiang, J.J. Yao, H.X. Deng, W.H. Li, Investigation on magnetorheological elastomers based on natural rubber, *Journal of Material Science* 42 (2007) 5483–5489.
[24] X. Zhang, W. Li, X.L. Gong, An effective permeability model to predict field-dependent modulus of magnetorheological elastomers, *Communications in Nonlinear Science and Numerical Simulation* 13 (2008) 1910–1916.
[25] H.X. Deng, X.-L. Gong, Application of magnetorheological elastomer to vibration absorber, *Communications in Nonlinear Science and Numerical Simulation* 13 (2008) 1938–1947.